Using Twelve Years of USGS Refraction Lines to Calibrate the Brocher and others (1997) 3D Velocity Model of the Bay Area

John Boatwright[1], Luke Blair[1] Rufus Catchings[1], Mark Goldman[1], Fabio Perosi[1], and Clare Steedman[1]

Open-File Report 2004-1282

2004

U.S. DEPARTMENT OF THE INTERIOR
U.S. GEOLOGICAL SURVEY

[1]U.S. Geological Survey, 345 Middlefield Road, MS 977, Menlo Park, CA 94025

Abstract

Campbell (1983) demonstrated that site amplification correlates with depths to the 1.0, 1.5, and 2.5 km/s S-wave velocity horizons. To estimate these depths for the Bay Area stations in the PEER/NGA database, we compare the depths to the 3.2 and 4.4 km/s P-wave velocities in the Brocher and others (1997) 3D velocity model with the depths to these horizons determined from 6 refraction lines shot in the Bay Area from 1991 to 2003. These refraction lines range from two recent 20 km lines that extend from Los Gatos to downtown San Jose, and from downtown San Jose into Alum Rock Park, to two older 200 km lines than run axially from Hollister up the San Francisco Peninsula to Inverness and from Hollister up the East Bay across San Pablo Bay to Santa Rosa. Comparison of these cross-sections with the Brocher and others (1997) model indicates that the 1.5 km/s S-wave horizon, which we correlate with the 3.2 km/s P-wave horizon, is the most reliable horizon that can be extracted from the Brocher and others (1997) velocity model. We determine simple adjustments to bring the Brocher and others (1997) 3.2 and 4.4 km/s P-wave horizons into an average agreement with the refraction results. Then we apply these adjustments to estimate depths to the 1.5 and 2.5 km/s S-wave horizons beneath the strong motion stations in the PEER/NGA database.

Introduction

Brocher et al. (1997) applied the method of Jachens and Moring (1990) to invert the isostatic gravity anomaly for the thickness of the Cenozoic sediments throughout the Bay Area. The inversion uses gravity observations made directly on basement and sediments and assumes a single density-depth function within the Cenozoic basins. The inversion also assumes vertical faults and cannot resolve overthrust geometries within the basins. They combined this sedimentary model with a geologic model of the major faults in the region to determine a 3D model that extends down to the Moho. By assigning velocity gradients to the basin fills and the bedrock blocks, they were able to assemble the first complete 3D Vp and Vs velocity model for the Bay Area.

The Brocher et al. (1997) 3D model is a remarkable product, and it has performed well as a 1st order model for seismic velocities in the Bay Area. However, the models for the Cenozoic basins depend explicitly on the average density-depth and velocity-depth functions determined by Brocher et al. (1997) and Tiballi and Brocher (1998) from industry borehole wells that were largely sited in the Livermore and San Pablo basins. Recently, we have re-picked and re-inverted 10 refraction lines shot by the USGS in the Bay Area from 1980 to 2003. The velocity cross-sections obtained from these refraction lines allow us to recalibrate the Brocher et al. (1997) velocity model.

Figure 1 shows the seven most recent refraction lines, along with the cutout volumes from the 3D model that we used for comparison. The black bars locate the cross-sections where we show direct comparisons of the models, with the Figures for these comparisons labeled.

Method of Comparison

The object of this report is to estimate the depths to the 1.0, 1.5, and 2.5 km/s S-wave velocities beneath the strong motion stations in the Bay Area. from the Brocher et al. (1997) model. In general, the S-wave velocities in the Brocher et al. (1997) model are generated from the P-wave velocities, which are prescribed as functions of depth in four different volumes. To calibrate the Brocher et al. (1997) estimates, we first determine that Vp velocities of 3.2 and 4.4 km/s correspond to Vs velocities of 1.5 and 2.5 km/s. We also find that we cannot resolve the Vs = 1.0 km/s horizon from the P-wave refraction results because of the marked variation of Vp/Vs between near-surface soil and rock. Then we compare the depths to these Vp velocities from the Brocher et al. (1997) model against the P-wave refraction results recently obtained by Catchings (see Addendum). In general, the Brocher et al. (1997) model is slower than the refraction models. We derive corrections for the Brocher et al. (1997) model that are linear functions of depth, and use these corrections to revise the depths to the Vs = 1.5 and 2.5 km/s horizons beneath the strong motion stations.

Figure 2 compares S-wave velocities obtained by Catchings et al. (2004) for the line running from Los Gatos to downtown San Jose to the cutout of the Brocher et al. (1997) model. The comparison is masked where the ray coverage is sparse. The contour lines show 1.0, 1.5, and 2.5 km/s S-wave

horizons from the refraction results, while the colored background indicates the same S-wave velocities in the Brocher et al. (1997) model. The fit of the 1.5 km/s horizon with the green-orange boundary is quite good, although the Brocher et al. (1997) model is almost always deeper.

In contrast, the fit of the 2.5 km/s boundary is poor and spatially variable. We assume that this misfit results from the lack of resolution of the deeper sections of the basins in the Brocher at al. (1997) model. This lack of resolution occurs for two reasons. First, the isostatic gravity anomaly from these sections is weaker because the density difference between the deeper sediments and the basement is smaller, and second, any consistent misfit of the assumed density function in the shallow section will project into a larger misfit in the deeper section.

Unfortunately, the Los Gatos line is the only refraction line on which S-waves could be picked and inverted. To incorporate the velocity structure obtained from the other refraction lines, it is necessary to compare P-wave velocities. For this comparison, we choose P-wave velocities of 2.4, 3.2, and 4.4 km/s as analogs to the S-wave velocities of 1.0, 1.5, and 2.5 km/s.

Our choice of Vp = 2.4 km/s as the analog for Vs = 1.0 km/s is derived by averaging Vp's that correspond to Vs =1.0 km/s from the shallow borehole results compiled by Boore (2003), shown in Figure 3. We note, however, that this result applies to shallow rock layers rather than buried sedimentary layers, for which Brocher et al. (1997) used the relation shown at the top of the plot. The marked difference between rock and sediment Vp/Vs, coupled with the sparse sampling of the Vp = 2.4 km/s horizon in the refraction lines obviates correcting the Vs = 1.0 km/s horizon from the Brocher et al. (1997) model using the P-wave refraction results.

Our choices of Vp = 3.2 and 4.4 km/s as analogs for Vs = 1.5 and 2.5 km/s are obtained by overlaying the Catchings et al. (2004) S-wave and P-wave results for the Los Gatos refraction line, and simply averaging the Vp estimates along the Vs = 1.5 and 2.5 contours. Catchings et al.'s (2004) Vp contours are plotted against the Brocher et al. (1997) velocities in Figure 4. We note that while the P-wave velocity of 3.2 km/s yields a good overall fit to the S-wave velocity of 1.5 km/s, the Vp/Vs ratio varies systematically along the eastern segment of this line.

Figures 5-9 show the comparison of the refraction P-wave velocity horizons with the P-wave velocities in the Brocher et al. (1997) model for the other cross-sections. Figure 5 shows the line across the Evergreen Basin that was shot in May 2003. The correspondence to the west of the basin, in the saddle underlying San Jose, is excellent, while the fit to the east is weaker. The Los Gatos and Evergreen lines, shot in 2000 and 2003, are the most densely sampled lines, with receivers at 50 m spacing. This dense spacing of receivers yields an excellent resolution of the near-surface velocity structure.

The receiver spacing for the 1991-1993 lines was about 1 km, which is significantly coarser than the 50 m spacing for the later lines. This coarse spacing yields a much poorer resolution of the near-surface velocity structure. Figure 6 shows an extreme example of this lack of resolution, for the so-called central section of the East-Bay line. Only the 4.4 km/s Vp contour can be discerned in this cross-section. The apparent variation in the Brocher et al. (1997) model results from the refraction line running along a volume boundary and the volumetric averaging used to determine the Brocher et al. (1997) model cross-sections.

Further north, on either side of San Pablo Bay, the P-wave horizons in Figure 7 are in much better agreement, although the refraction lines do not image the deeper basin structure inferred from the gravity inversion. The masked area in the middle of the cross-section underlies San Pablo Bay, where a set of OBS instruments failed to record usable signals.

The eastern section of the Cross-Bay line, shown in Figure 8, is the only cross-section where the 4.4 km/s P-wave velocity obtained by the refraction line is clearly deeper that estimated by Brocher et al. (1997). The low velocities associated with the Livermore basin appear to start as far west as the Hayward fault. However, the 3.2 km/s contour is still shallower than the Brocher et al. (1997) estimate, reaffirming our choice of this intermediate velocity as the most stable marker.

Finally, the western section of the Cross-Bay line is shown in Figure 9. Here the refraction profile does not see the bedrock velocity contrast that Brocher et al. (1997) incorporate across the San Andreas fault. Equally surprising is the apparent basement saddle that underlies the southern San Francisco Bay, on the right of the cross section.

Adjusting the Brocher et al. (1997) Model

To estimate depths to the 1.5 km/s S-wave horizon, we will adjust the Brocher et al. (1997) model as simply as possible. First, we regress the difference between the 3.2 km/s depths from the two models as a linear function of depth, that is, as

$$\chi^2 = \sum \left(z_{3.2}^R(x_i) - b z_{3.2}^B(x_i) - c \right)^2 \qquad (1)$$

where $z_{3.2}^B(x_i)$ is the depth of the 3.2 km/s P-wave velocity in the Brocher et al. (1997) model, and $z_{3.2}^R(x_i)$ is the depth obtained from the refraction studies. Sample points x_i were chosen at 1 km spacing for the Los Gatos and Evergreen lines, and 3 km spacing for the Peninsula, East Bay, and Cross Bay lines. For the Peninsula, East Bay and Cross Bay lines, we did not use the $z_{3.2}^R(x_i)$ estimates where they were above the elevation of the free surface. These misestimates result from the lack of resolution of the near-surface velocities and the smoothing of the tomographic inversion.

The simple linear parameterization as a function of depth in equation (1) corresponds adequately with the velocity-depth functions assumed by Brocher's et al. (1997). Figure 10 shows the comparison of $z_{3.2}^B(x_i)$ and $z_{3.2}^R(x_i)$. Because the Brocher et al. (1997) model is a series of bounded volumes with prescribed rules for the velocity as a function of depth, the 3.2 km/s P-wave velocity occurs only at depths of about 0.1, 0.7, and 1.6 km, depending on the volume the refraction line transects. Slight variations from these depths occur because the P-wave velocity is being sampled within a volume around the refraction lines. Regressing $z_{3.2}^R$ on $z_{3.2}^B$ yields the result

$$z_{3.2}^R = 0.164 + 0.352\, z_{3.2}^B \qquad (2)$$

with the associated uncertainties

$$\sigma(z_{3.2}^R) \approx 0.65\, z_{3.2}^R \, . \qquad (3)$$

Similarly, regressing $z_{4.4}^R$ on $z_{4.4}^B$ yields

$$z_{4.4}^{R} = 0.679 + 0.417 z_{4.4}^{B} \quad (4)$$

with the associated uncertainties

$$\sigma(z_{4.4}^{R}) \approx 0.45 z_{4.4}^{R} . \quad (5)$$

Table 1 contains the Excel Worksheet for the PEER/NGA stations that fall within the area of the 3D velocity model. We use the adjustments given above to correct the depths of the 3.2 and 4.4 km/s P-wave horizons obtained from the Brocher et al. (1997) model. We also estimate the uncertainty of these depths.

In addition, we have estimated the depth to these horizons directly from the refraction data for those stations within 5 km of a refraction line. More than half (71 out of 133) of the stations are sufficiently close to a refraction line to directly estimate the depth to the Vp = 3.2 and 4.4 km/s horizon. However, for 58 of these 71 stations, the Vp = 3.2 km/s horizon was determined from the tomographic inversions of the P-wave arrival times to be above the elevation of the station. These misestimates are generally derived for the stations near the Peninsula, East Bay, and Cross Bay lines, and result from the lack of resolution of near-surface velocities and the smoothing of the tomographic inversion. We consider these estimates of $z_{3.2}^{R}$ to be relatively weak and leave the EXCEL element empty.

Finally, in Table 2, we compile estimates of the depth to the Vs = 1.0 and 1.5 km/s horizons for seven strong motion stations that are sufficiently close to boreholes that penetrate to these velocities. We also indicate the number of the borehole assigned by Boore (2003). Unfortunately, there are no direct comparisons of depth to Vp = 3.2 km/s from refraction lines and borehole estimates of depth to Vs = 1.5 km/s. In general, the Brocher et al. (1997) estimate of the depth to Vp = 3.2 km/s for these stations was 0.64 km, which we have corrected to 0.39 km. This estimate appears quite deep, relative to these borehole sites underlain by shallow rocks, but we presume that the requirement that the boreholes directly sample Vs = 1.0 km/s material introduces a strong sampling bias. We note, as well, that this compilation may be incomplete, as it is derived from Boore's (2003) compilation of borehole velocity results, and does not include all the borehole velocity structures that have been obtained in the Bay Area.

Conclusions

We have compared the velocities in the Brocher et al. (1997) 3D model to the velocity structures obtained from the inversion of more than 500 km of refraction lines shot in the Bay Area from 1991 to 2003. In general, the velocities in the Brocher 3D model are slower than the velocities inferred from the refraction lines. We have determined simple corrections, that is, $\Delta z(z)$, for the depths to the Vp = 3.2 and 4.4 km/s horizons estimated from the Brocher et al. 3D model and compiled these corrected depths for the strong motion stations in the Bay Area in the PEER/NGA database. We have also compiled the depths to these horizons beneath those stations within 5 km of the refraction lines, where these velocity structures can be inverted directly. Finally, we have added a table showing the depth to Vs = 1.0 and 1.5 km/s for seven stations where it was obtained directly from boreholes.

Acknowledgements

The authors are grateful for the rapid and thorough reviews of this report provided by Paul Spudich and Shane Detweiler. The online database of borehole velocities compiled by Dave Boore provided a critical grounding for many of the geophysical interpretations in this paper.

This project was sponsored by the Pacific Earthquake Engineering Research Center's Program of Applied Earthquake Engineering Research of Lifeline Systems supported by the California Energy Commission, California Department of Transportation, and the Pacific Gas & Electric Company. The financial support of the PEARL sponsor organizations including the Pacific Gas & Electric Company, the California Energy Commission, and the California Department of Transportation is acknowledged. This work made use of Earthquake Engineering Research Centers Shared Facilities supported by the National Science Foundation under Award Number EEC-9701568.

Commission, the State of California, its employees, Contractors and subcontractors make no warranty, express or implied, and assume no legal liability for the information in this report; nor does any party represent that the use of this information will not infringe upon privately owned rights. This report has not been approved or disapproved by the Commission nor has the commission passed upon the accuracy or adequacy of the information in this report.

Bibliography

Boore, D.M., (2003). P- and S- Velocities from Surface-to-Borehole Logging, http://quake.wr.usgs.gov/~boore/data_online.htm.

Brocher, T.M., E.E. Brabb, R.D. Catchings, G.S. Fuis, T.E. Fumal, R.C. Jachens, A.S. Jayko, R.E. Kayen, R.J. McLaughlin, Tom Parsons, M.J. Rymer, R.G. Stanley, C.M. Wentworth, (1997). A crustal-scale 3-D seismic velocity model for the San Francisco Bay area, California, *Eos*, vol.78, no.46, Suppl., pp.435-436.

Campbell, Kenneth W, (1983). The effects of site characteristics on near-source recordings of strong-ground motion. Hays, Walter W. (ed.), Kitzmiller, Carla, and Darnell, Diana, *A workshop on site-specific effects of soil and rock on ground motion and the implications for earthquake-resistant design*, *Open-file Report* 83-0845.

Catchings, R.D., G. Gandhok, M.R. Goldman, R. Hansen, and R. McLaughlin (2004). Basin structure and velocities from the 2000 Santa Clara Seismic Investigation (SCSI) as related to earthquake hazards and water resources, western Santa Clara Valley, California, *U.S. Geological Survey Open-File Report* 04-xxx.

Jachens, R.C., and B.C. Moring (1990). Maps of the thickness of Cenozoic deposits and the isostatic residual gravity over basement for Nevada, *U.S. Geological Survey Open-File Report* 90-496, 11 p.

Tiballi, C.A., and T.M. Brocher (1998). Compilation of 71 additional sonic and density logs from 59 oil test wells in the San Francisco Bay area, *U.S. Geological Survey Open-File Report* 98-615, 131 p.

Table Captions

Table 1. Estimated depths to Vp = 3.2 and 4.4 km/s horizons beneath the Bay Area stations in the PEER/NGA database. The sequence #, station #, and descriptive station name are taken from the PEER/NGA database, although some station names have been edited for brevity. The station elevation (Elev) is in km. The first column labeled as (Brchr Vp) contains the P-wave velocity in km/s for the horizon whose depth is given in the following (Brchr Z(3.2)) column. The (Brchr Z(3.2)) column contains the Brocher et al. (1997) estimate of depth in km of the Vp = 3.2 km/s horizon beneath the station. The column labeled (Brchr Z'(3.2)) contains the adjusted estimate of the depth in km to the Vp = 3.2 km/s horizon obtained from equation (2). The column labeled (Brchr dZ(3.2)) contains the uncertainty in km obtained from equation (3). Similarly, the second column labeled as (Brchr Vp) contains the P-wave velocity in km/s for the horizon whose depth is given in the following (Brchr Z(4.4)) column. The column labeled (Brchr Z(4.4)) contains the Brocher et al. (1997) estimate of the depth in km to the Vp = 4.4 km/s horizon beneath the station. The column labeled (Brchr Z'(4.4)) contains the adjusted estimate of the depth in km to the Vp = 4.4 km/s horizon obtained from equation (4). The column labeled (Brchr dZ(4.4)) contains the uncertainty in km obtained from equation (5). The columns labeled (Rfrct Z(3.2)) and (Rfrct Z(4.4)) contain the estimates of the depths in km to the Vp = 3.2 and 4.4 km/s horizons inferred obtained directly from refraction lines that fall within 5 km of the station. Finally, the column labeled (Offset) contains the offset in km of the strong motion station from the refraction line used to estimate (Rfrct Z(3.2)) and (Rfrct Z(4.4))

Table 2. Depths to the Vs = 1.0 and 1.5 km/s horizons beneath seven Bay Area stations in the PEER/NGA database, obtained directly from borehole logging.. The sequence #, station #, and descriptive station name are taken from the PEER/NGA database. The column labeled (Boore #) contains the number of the borehole in the Boore (2003) database. The columns labeled (Borehole Z(Vs=1.0)) and (Borehole Z(Vs=1.5)) contain the depths in km to the Vs = 1.0 and 1.5 km/s horizons determined in the boreholes. The column labeled (Refraction Z(Vp=4.4)) contains the estimates of the depth in km of the Vp = 4.4 km/s horizon inferred from the refraction line. No estimates of the depth to the Vp = 3.2 km/s horizon were available for these stations. Finally, the column labeled (Distance from Line) contains the offset of the station from the refraction line.

Table 1

Seq #	Sta #	Station Name	Latitude	Longitude	Elev	Brchr Vp	Brchr Z(3.2)	Brchr Z'(3.2)	Brchr dZ(3.2)	Brchr Vp	Brchr Z(4.4)	Brchr Z'(4.4)	Brchr dZ(4.4)	Rfrct Z(3.2)	Rfrct Z(4.4)	Offset
427	57066	Agnews State Hospital	37.39	-121.95		3.17	0.67	0.40	0.26	4.41	2.25	1.62	0.73			
1157	1756	Alameda - Oakland Air	37.73	-122.25		3.13	0.65	0.39	0.26	4.41	2.25	1.62	0.73			
1156	1755	Alameda Fire Station #1	37.76	-122.24		3.13	0.65	0.39	0.26	4.41	2.25	1.62	0.73			
569	99999	Alameda Naval Air Stn	37.78	-122.30		3.13	0.65	0.39	0.26	4.41	2.25	1.62	0.73			
170	1652	Anderson Dam (Dwnstrm)	37.16	-121.62	0.18	3.16	0.66	0.40	0.26	4.41	2.25	1.62	0.73		2.41	1.59
171	1652	Anderson Dam (L Abut)	37.16	-121.62	0.18	3.16	0.66	0.40	0.26	4.41	2.25	1.62	0.73		2.41	1.59
458	58373	APEEL 10 - Skyline	37.46	-122.34		3.15	0.65	0.39	0.26	4.41	2.25	1.62	0.73			
460	58376	APEEL 1E - Hayward	37.62	-122.13		3.14	0.65	0.39	0.26	4.41	2.25	1.62	0.73			
119	1002	APEEL 2 - Redwood City	37.52	-122.25	0.00	3.13	0.64	0.39	0.25	4.41	2.25	1.62	0.73		0.00	2.76
462	58393	APEEL 2E Hayward Muir	37.65	-122.08		3.13	0.64	0.39	0.25	4.41	2.25	1.62	0.73			
450	58219	APEEL 3E Hayward CSUH	37.65	-122.06	0.13	3.13	0.49	0.34	0.22	4.30	1.40	1.26	0.57		1.49	3.66
461	58378	APEEL 7 - Pulgas	37.48	-122.31	0.12	3.13	0.65	0.39	0.26	4.41	2.25	1.62	0.73		0.00	4.24
144	1161	APEEL 9 - Crystal Springs	37.47	-122.32		3.13	0.65	0.39	0.26	4.41	2.25	1.62	0.73			
1448	47750	Aptos - Sea Cliff Array	36.97	-121.90	0.02	3.29	0.12	0.21	0.13	4.46	1.00	1.10	0.49	0.30	1.78	1.38
455	58262	Belmont - Envirotech	37.51	-122.30	0.15	3.13	0.64	0.39	0.25	4.41	2.25	1.62	0.73		0.55	1.99
1160	1760	Benicia Fire Station #1	38.05	-122.15		4.05	0.25	0.25	0.16	4.29	1.29	1.22	0.55			
463	58471	Berkeley LBL	37.87	-122.24	0.24	3.21	1.62	0.73	0.48	4.38	3.63	2.19	0.99		2.28	4.22
14	13	BRAN	37.04	-121.98		3.29	0.12	0.21	0.13	4.47	1.00	1.10	0.49			
400	47125	Capitola	36.97	-121.95	0.00	3.29	0.12	0.21	0.13	4.46	1.00	1.10	0.49	0.28	1.81	2.41
424	57007	Corralitos	37.05	-121.80	0.42	3.21	1.62	0.73	0.48	4.39	3.13	1.98	0.89		1.11	1.73
436	57504	Coyote Lake Dam Dwnstrm	37.12	-121.55	0.21	3.21	0.68	0.40	0.26	4.41	2.25	1.62	0.73		2.86	1.55
431	57217	Coyote Lake Dam SW Abut	37.11	-121.55	0.24	3.17	0.66	0.40	0.26	4.41	2.25	1.62	0.73		2.89	1.32
1141	1720	Cupertino - Sunnyvale Rod	37.29	-122.08	0.22	3.13	0.64	0.39	0.25	4.41	2.25	1.62	0.73		0.27	0.95
1137	1690	Danville Fire Station	37.81	-121.99		3.21	1.62	0.73	0.48	4.38	3.75	2.24	1.01			
146	1265	Del Valle Dam (Toe)	37.62	-121.75		3.21	1.62	0.73	0.48	4.40	2.87	1.88	0.84			
1136	1689	Dublin - Fire Station	37.70	-121.93		3.21	1.62	0.73	0.48	4.38	3.75	2.24	1.01			
1460	58664	Dumbarton Bridge West	37.49	-122.13	0.00	3.13	0.65	0.39	0.26	4.41	2.25	1.62	0.73		1.88	3.59
1144	1737	El Cerrito - Mira Vista CC	37.93	-122.30	0.20	3.20	1.48	0.68	0.45	4.39	3.43	2.11	0.95		2.94	4.45
459	58375	Foster City - APEEL 1	37.54	-122.23		3.13	0.64	0.39	0.25	4.41	2.25	1.62	0.73			
1154	1753	Foster City - Bowditch Sch	37.56	-122.24		3.13	0.64	0.39	0.25	4.41	2.25	1.62	0.73			
1456	57784	Fremont - 2 Story City Lbr	37.55	-121.97	0.02	3.18	0.67	0.40	0.26	4.41	2.25	1.62	0.73		0.30	3.59

Seq #	Sta #	Station Name	Latitude	Longitude	Elev	Brchr Vp	Brchr Z(3.2)	Brchr Z'(3.2)	Brchr dZ(3.2)	Brchr Vp	Brchr Z(4.4)	Brchr Z'(4.4)	Brchr dZ(4.4)	Rfrct Z(3.2)	Rfrct Z(4.4)	Offset Offset
1457	57948	Fremont - 2 Story Ind Bldg	37.47	-121.92		3.13	1.50	0.69	0.45	4.41	2.25	1.62	0.73			
1151	1750	Fremont - Coyote Hills	37.55	-122.09		3.13	0.65	0.39	0.26	4.41	2.25	1.62	0.73			
177	1686	Fremont - Emerson Court	37.53	-121.92	0.06	4.04	1.11	0.55	0.36	4.39	2.14	1.57	0.71		1.24	4.45
426	57064	Fremont - MSJ	37.53	-121.91	0.09	3.13	1.50	0.69	0.45	4.41	2.25	1.62	0.73		1.11	0.99
399	47006	Gilroy - Gavilan Coll.	36.97	-121.56		3.12	0.64	0.39	0.25	4.41	2.25	1.62	0.73			
435	57476	Gilroy - Historic Bldg.	37.00	-121.56		3.13	0.65	0.39	0.26	4.41	2.25	1.62	0.73			
406	47379	Gilroy Array #1	36.97	-121.57		3.13	0.65	0.39	0.26	4.41	2.25	1.62	0.73			
407	47380	Gilroy Array #2	36.98	-121.55		3.13	0.65	0.39	0.26	4.41	2.25	1.62	0.73			
408	47381	Gilroy Array #3	36.98	-121.53		3.13	0.65	0.39	0.26	4.41	2.25	1.62	0.73			
432	57382	Gilroy Array #4	37.00	-121.52	0.05	3.13	0.64	0.39	0.25	4.41	2.25	1.62	0.73		2.43	3.81
433	57383	Gilroy Array #6	37.02	-121.48	0.32	3.20	1.60	0.73	0.47	4.42	2.29	1.63	0.74		2.65	0.54
434	57425	Gilroy Array #7	37.03	-121.43	0.31	3.12	0.65	0.39	0.26	4.40	2.87	1.88	0.84	0.38	2.72	4.64
176	1678	Golden Gate Bridge	37.80	-122.47		3.13	0.65	0.39	0.26	4.41	2.25	1.62	0.73			
142	1117	Golden Gate Park	37.77	-122.48	0.06	3.13	0.65	0.39	0.26	4.41	2.25	1.62	0.73		1.37	3.67
1462	58964	Half Moon Bay - Array	37.36	-122.39		3.21	1.62	0.73	0.48	4.38	3.75	2.24	1.01			
430	57191	Halls Valley	37.33	-121.71	0.46	3.13	0.65	0.39	0.26	4.40	2.40	1.68	0.76		1.38	2.54
464	58498	Hayward - BART Sta	37.67	-122.08	0.03	3.13	0.65	0.39	0.26	4.41	2.25	1.62	0.73		1.40	4.72
1155	1754	Hayward FS #1	37.67	-122.08	0.02	3.13	0.63	0.39	0.25	4.29	1.37	1.25	0.56		1.39	4.24
1172	1797	Hollister - Airport #3	36.89	-121.40	0.06	3.91	1.47	0.68	0.44	4.40	2.77	1.83	0.83		2.40	1.85
1131	1575	Hollister - City Hall Annex	36.85	-121.40	0.08	3.18	1.58	0.72	0.47	4.43	2.30	1.64	0.74		3.68	1.67
128	1032	Hollister - SAGO Vault	36.76	-121.44		3.29	0.12	0.21	0.13	4.46	1.00	1.10	0.49			
409	47524	Hollister - South & Pine	36.84	-121.39	0.08	3.13	1.50	0.69	0.45	4.40	2.65	1.78	0.80		3.68	1.58
127	1028	Hollister City Hall	36.85	-121.40	0.08	3.13	1.50	0.69	0.45	4.41	2.40	1.68	0.76		3.68	1.63
174	1656	Hollister Diff Array #1	36.88	-121.41	0.07	3.13	1.50	0.69	0.45	4.41	2.25	1.62	0.73		2.46	2.66
174	1656	Hollister Diff Array #3	36.88	-121.41	0.07	3.13	1.50	0.69	0.45	4.41	2.25	1.62	0.73		2.46	2.66
174	1656	Hollister Diff Array #4	36.88	-121.41	0.07	3.13	1.50	0.69	0.45	4.41	2.25	1.62	0.73		2.46	2.66
174	1656	Hollister Diff Array #5	36.88	-121.41	0.07	3.13	1.50	0.69	0.45	4.41	2.25	1.62	0.73		2.46	2.66
174	1656	Hollister Diff. Array	36.88	-121.41	0.07	3.13	1.50	0.69	0.45	4.41	2.25	1.62	0.73		2.46	2.66
1132	1590	Larkspur Ferry Terminal	37.94	-122.50		3.13	0.65	0.39	0.26	4.41	2.25	1.62	0.73			
17	16	LGPC	37.17	-122.01	0.44	3.21	1.55	0.71	0.46	4.39	3.34	2.07	0.93	0.16	0.72	0.38
437	0	Livermore - Fagundas	37.75	-121.77	0.19	3.21	1.62	0.73	0.48	4.38	3.75	2.24	1.01	0.00	1.83	1.36
438	0	Livermore - Morgan Park	37.81	-121.79	0.62	4.05	0.25	0.25	0.16	4.29	1.29	1.22	0.55	0.31	2.15	5.00
1451	57180	Los Gatos - Lexington Dam	37.20	-121.99	0.21	3.13	0.65	0.39	0.26	4.41	2.25	1.62	0.73	0.19	1.06	0.21
1139	1697	Los Gatos - Los Altos Rod	37.23	-122.10		3.21	1.62	0.73	0.48	4.38	3.75	2.24	1.01			

Seq #	Sta #	Station Name	Latitude	Longitude	Elev	Brchr Vp	Brchr Z(3.2)	Brchr Z'(3.2)	Brchr dZ(3.2)	Brchr Vp	Brchr Z(4.4)	Brchr Z'(4.4)	Brchr dZ(4.4)	Rfrct Z(3.2)	Rfrct Z(4.4)	Offset Offset
1458	58233	Lower Crystal Springs	37.52	-122.36	0.06	3.13	0.64	0.39	0.25	4.41	2.25	1.62	0.73		1.32	4.50
1167	1784	Menlo Park - USGS #11	37.45	-122.17	0.01	3.13	0.65	0.39	0.26	4.41	2.25	1.62	0.73		3.74	3.41
1149	1745	Menlo Park - USGS #15	37.45	-122.16	0.01	3.13	0.64	0.39	0.25	4.41	2.25	1.62	0.73		3.74	3.23
405	47377	Monterey City Hall	36.59	-121.89		3.29	0.12	0.21	0.13	4.46	1.00	1.10	0.49			
1158	1758	Morgan Hill - El Toro FS	37.14	-121.66		3.13	0.65	0.39	0.26	4.41	2.25	1.62	0.73			
1162	1762	Novato Fire Station #1	38.09	-122.56		3.13	0.65	0.39	0.26	4.41	2.25	1.62	0.73			
1152	1751	Novato Fire Station #4	38.06	-122.53		3.13	0.64	0.39	0.25	4.41	2.25	1.62	0.73			
1459	58472	Oakland - Outer Harbor	37.81	-122.31		3.13	0.64	0.39	0.25	4.41	2.25	1.62	0.73			
453	58224	Oakland - Title & Trust	37.80	-122.26		3.13	0.65	0.39	0.26	4.41	2.25	1.62	0.73			
456	58264	Palo Alto - 1900 Embar	37.45	-122.11	0.00	3.13	0.64	0.39	0.25	4.41	2.25	1.62	0.73		2.86	0.89
1169	1787	Palo Alto - FS #7 SLAC	37.41	-122.20	0.09	3.14	0.65	0.39	0.26	4.41	2.25	1.62	0.73			1.27
162	1601	Palo Alto - SLAC Lab	37.42	-122.21	0.10	3.13	0.65	0.39	0.26	4.41	2.25	1.62	0.73		0.00	1.44
457	58338	Piedmont Jr High	37.82	-122.23		3.13	0.65	0.39	0.26	4.40	2.21	1.60	0.72			
1138	1691	Pleasant Hill FS #2	37.92	-122.07		3.21	1.62	0.73	0.48	4.38	3.75	2.24	1.01			
1168	1785	Pleasanton FS #1	37.66	-121.87	0.10	3.21	1.62	0.73	0.48	4.38	3.75	2.24	1.01		1.56	1.57
439	58043	Point Bonita	37.82	-122.52	0.04	3.13	0.65	0.39	0.26	4.41	2.25	1.62	0.73		0.20	3.93
1150	1749	Richmond - Point Molate	37.95	-122.41		3.13	0.65	0.39	0.26	4.41	2.25	1.62	0.73			
465	58505	Richmond City Hall	37.93	-122.34		3.13	0.65	0.39	0.26	4.41	2.25	1.62	0.73			
1142	1722	Richmond Rod & Gun Club	37.97	-122.36		3.18	1.58	0.72	0.47	4.41	2.25	1.62	0.73			
403	47189	SAGO South - Surface	36.75	-121.39		3.28	0.17	0.22	0.15	4.46	1.61	1.35	0.61			
1449	47762	Salinas - County Hospital	36.69	-121.63		4.22	1.00	0.52	0.34	4.61	1.14	1.15	0.52			
402	47179	Salinas - John & Work	36.67	-121.64		3.13	1.50	0.69	0.45	4.66	1.25	1.20	0.54			
1143	1735	San Francisco - 9th Circ	37.77	-122.41		3.13	0.65	0.39	0.26	4.41	2.25	1.62	0.73			
1133	1675	San Francisco - FS #17	37.72	-122.38		3.13	0.64	0.39	0.25	4.41	2.25	1.62	0.73			
1166	1774	San Francisco - FS #2	37.76	-122.50	0.01	3.13	0.65	0.39	0.26	4.41	2.25	1.62	0.73		1.21	1.36
1146	1741	San Francisco - Marina	37.80	-122.44		3.13	0.65	0.39	0.26	4.41	2.25	1.62	0.73			
1453	57600	San Jose - Emory & Bell	37.32	-121.93	0.03	3.99	1.31	0.63	0.41	4.41	2.25	1.62	0.73	0.76	1.97	1.31
1454	57604	San Jose - S Clara Bldg	37.35	-121.90	0.01	3.33	0.75	0.43	0.28	4.41	2.25	1.62	0.73	0.53	1.95	1.74
1452	57563	San Jose - Santa Teresa	37.21	-121.80	0.22	3.13	0.65	0.39	0.26	4.41	2.25	1.62	0.73	0.38	1.66	2.42
1147	1742	San Jose - Weather Sta	37.35	-121.90	0.01	3.19	0.68	0.40	0.26	4.41	2.25	1.62	0.73	0.51	1.95	1.39
401	47126	San Juan Bautista	36.86	-121.54	0.05	3.24	1.00	0.52	0.34	4.40	3.07	1.96	0.88		3.65	2.09
172	1655	San Justo Dam (L Abut)	36.82	-121.44	0.14	3.21	1.62	0.73	0.48	4.49	2.57	1.75	0.79		3.73	2.27
173	1655	San Justo Dam (R Abut)	36.82	-121.44	0.14	3.21	1.62	0.73	0.48	4.49	2.57	1.75	0.79		3.73	2.27
429	57187	San Ramon - Eastman	37.72	-121.92		3.21	1.62	0.73	0.48	4.38	3.75	2.24	1.01			

Seq #	Sta #	Station Name	Latitude	Longitude	Elev	Brchr Vp	Brchr Z(3.2)	Brchr Z'(3.2)	Brchr dZ(3.2)	Brchr Vp	Brchr Z(4.4)	Brchr Z'(4.4)	Brchr dZ(4.4)	Rfrct Z(3.2)	Rfrct Z(4.4)	Offset Offset
428	57134	San Ramon Fire Station	37.78	-121.98		3.21	1.62	0.73	0.48	4.38	3.75	2.24	1.01			
1455	57748	Santa Clara - 237/Alviso	37.42	-121.97		3.13	0.64	0.39	0.25	4.41	2.25	1.62	0.73			
1450	48906	Santa Cruz - Co Office	36.97	-122.02		3.29	0.12	0.21	0.13	4.46	1.00	1.10	0.49			
440	58065	Saratoga - Aloha Ave	37.25	-122.03	0.16	3.13	0.65	0.39	0.26	4.41	2.25	1.62	0.73		0.23	0.25
454	58235	Saratoga - W Valley Coll.	37.26	-122.00	0.11	3.21	1.61	0.73	0.47	4.39	3.14	1.99	0.89		0.18	1.86
454	58235	Saratoga - WVC E Wall	37.26	-122.00	0.11	3.21	1.61	0.73	0.47	4.39	3.14	1.99	0.89		0.18	1.86
454	58235	Saratoga - WVC NE	37.26	-122.00	0.11	3.21	1.61	0.73	0.47	4.39	3.14	1.99	0.89		0.18	1.86
454	58235	Saratoga - WVC SE	37.26	-122.00	0.11	3.21	1.61	0.73	0.47	4.39	3.14	1.99	0.89		0.18	1.86
454	58235	Saratoga - WVC Wall	37.26	-122.00	0.11	3.21	1.61	0.73	0.47	4.39	3.14	1.99	0.89		0.18	1.86
445	58132	SF - Cliff House	37.77	-122.51	0.00	3.13	0.64	0.39	0.25	4.41	2.25	1.62	0.73		0.97	1.88
443	58130	SF - Diamond Heights	37.74	-122.43	0.14	3.13	0.65	0.39	0.26	4.41	2.25	1.62	0.73		2.04	4.95
444	58131	SF - Pacific Heights	37.79	-122.42		3.13	0.65	0.39	0.26	4.41	2.25	1.62	0.73			
451	58222	SF - Presidio	37.79	-122.45		3.13	0.65	0.39	0.26	4.41	2.25	1.62	0.73			
448	58151	SF - Rincon Hill	37.78	-122.39		3.13	0.65	0.39	0.26	4.41	2.25	1.62	0.73			
446	58133	SF - Telegraph Hill	37.80	-122.40		3.13	0.65	0.39	0.26	4.41	2.25	1.62	0.73			
452	58223	SF Intern. Airport	37.62	-122.39	0.00	3.13	0.65	0.39	0.26	4.41	2.25	1.62	0.73		1.73	0.74
404	47315	SJB Overpass, 3	36.86	-121.57	0.12	3.19	1.60	0.73	0.47	4.51	1.04	1.11	0.50		3.47	3.15
404	47315	SJB Overpass, 5	36.86	-121.57	0.12	3.19	1.60	0.73	0.47	4.51	1.04	1.11	0.50		3.47	3.15
466	58539	South SF, Sierra Pt.	37.67	-122.38	0.01	3.13	0.64	0.39	0.25	4.41	2.25	1.62	0.73		2.12	3.57
18	17	Stanford Park. Garage	37.43	-122.17	0.02	3.14	0.65	0.39	0.26	4.41	2.25	1.62	0.73	0.00	5.31	1.58
178	1695	Sunnyvale - Colton Ave.	37.40	-122.02		3.13	0.65	0.39	0.26	4.41	2.25	1.62	0.73			
1135	1688	Sunol - Forest FS	37.59	-121.88		3.21	1.62	0.73	0.48	4.29	1.40	1.26	0.57			
1134	1684	Sunol - Ohlone Wilderness	37.51	-121.83	0.12	3.12	0.64	0.39	0.25	4.35	2.19	1.59	0.72		0.20	4.76
441	58117	Treasure Island	37.82	-122.37		3.13	0.64	0.39	0.25	4.41	2.25	1.62	0.73			
441	58642	Treasure Island Array	37.82	-122.37		3.13	0.64	0.39	0.25	4.41	2.25	1.62	0.73			
16	15	UCSC	37.00	-122.06		3.29	0.12	0.21	0.13	4.46	1.00	1.10	0.49			
447	58135	UCSC Lick Observatory	37.00	-122.06		3.29	0.12	0.21	0.13	4.46	1.00	1.10	0.49			
1145	1739	Union City - Masonic	37.60	-122.00	0.07	3.13	0.63	0.39	0.25	4.31	1.54	1.32	0.59			2.91
1159	1759	Vallejo FS #1	38.10	-122.24		4.05	0.25	0.25	0.16	4.29	1.29	1.22	0.55			
15	14	WAHO	36.97	-121.99		3.29	0.12	0.21	0.13	4.46	1.00	1.10	0.49			
442	58127	Woodside	37.42	-122.25	0.11	3.13	0.65	0.39	0.26	4.41	2.25	1.62	0.73			4.15
1153	1752	Woodside - Filoli Center	37.46	-122.30	0.12	3.13	0.65	0.39	0.26	4.41	2.25	1.62	0.73			4.96
449	58163	Yerba Buena Island	37.80	-122.36		3.13	0.64	0.39	0.25	4.41	2.25	1.62	0.73			

Table 2

Seq_no	Sta_no	Station Name	Latitude	Longitude	Elevation	Boore #	Borehole Z(Vs=1.0)	Borehole Z(Vs=1.5)	Refraction Z(Vp=4.4)	Distance from Line
455	58262	Belmont - Envirotech	37.51	-122.30	0.15	3	0.012		0.55	1.99
1141	1720	Cupertino - Sunnyvale Rod & Gun	37.29	-122.08	0.22	157	0.008		0.27	0.95
406	47379	Gilroy Array #1	36.97	-121.57		192	0.003	0.010		
464	58498	Hayward - BART Sta	37.67	-122.08	0.03	137	0.013		1.40	4.72
1155	1754	Hayward Fire - Station #1	37.67	-122.08	0.02	137	0.013		1.39	4.24
443	58130	SF - Diamond Heights	37.74	-122.43	0.14	178	0.008		2.04	4.95
1145	1739	Union City - Masonic Home	37.60	-122.00	0.07	168	0.013			2.91

Figure Captions

Figure 1. Bay Area velocity model and seismic refraction lines. The extent of the Bay Area velocity model is indicated by the gray outline. The seismic refraction lines are plotted as colored lines surrounded by cutouts. The cutouts indicate the sections of the Brocher et al. (1997) model used for comparison with the refraction results. The cross-sections plotted in Figures 2 and 4-9 are indicated by the black bars and labeled with the number of the Figure.

Figure 2. Comparison of S-wave velocities for the Los Gatos line. The Brocher et al. (1997) model is plotted in solid colors, with color changes indicating the Vs = 1.0, 1.5, and 2.5 km/s horizons. The refraction results from Catchings et al. (2004) are shown as solid lines that are labeled. The plot is masked where the ray coverage of the refraction inversion is too sparse to resolve the velocity structure.

Figure 3. Vp/Vs from 38 shallow boreholes with S-wave layer velocities in the range $0.9 < Vs < 1.3$ km/s. The Vp and Vs estimates were derived independently by Boore (2003): this range of Vs is appropriate for near-surface rock layers. The straight line plotted on the graph shows the Vp/Vs ratio used by Brocher et al. (1997) for average Cenozoic sediments.

Figure 4. Comparison of P-wave velocities for the Los Gatos line. The Brocher et al. (1997) model is plotted in solid colors, with color changes indicating the Vp = 2.4, 3.2, and 4.4 km/s horizons. The refraction results from Catchings et al. (2004) are shown as solid lines that are labeled. The plot is masked where the ray coverage of the refraction inversion is too sparse to resolve the velocity structure.

Figure 5. Comparison of P-wave velocities for the Evergreen (east San Jose) line. The representation of the models is the same as in Figure 4. The fit of the Vp = 3.2 km/s horizon is excellent to the west of the Evergreen basin, but poor to the east.

Figure 6. Comparison of P-wave velocities for the central section of the East-Bay line. The representation of the models is the same as in Figure 4. The fit of the Vp = 4.4 km/s horizon is adequate, while the Vp = 3.2 km/s horizon (not plotted) is much shallower than the color change between the green and orange colors.

Figure 7. Comparison of P-wave velocities for the San Pablo Bay section of the East-Bay line. The representation of the models is the same as in Figure 4. The masked area is underneath San Pablo Bay. The fit of the Vp = 3.2 km/s horizon is excellent to the north of San Pablo Bay. The ~3 km deep sedimentary basins inferred from the gravity on both sides of the bay are not imaged by the seismic refraction.

Figure 8. Comparison of P-wave velocities for the eastern section of the Cross-Bay line. The representation of the two models is the same as in Figure 4. The eastern part of this line shows the Livermore basin, which appears as a 4 km thick section of low velocity sediment. This is the only refraction line that obtains slower velocities than the Brocher et al. (1997) model. Even in the Livermore basin, however, the depth to the Vp = 3.2 km/s horizon obtained from the refraction is 1 km shallower than that Inferred by Brocher et al. (1997).

Figure 9. Comparison of P-wave velocities for the western section of the Cross-Bay line. The representation of the two models is the same as in Figure 4. The refraction line does not see the velocity step across the San Andreas fault incorporated by Brocher et al. (1997) into their model.

Figure 10. Comparison of the depths to the Vp = 3.2 km/s horizon from the Brocher et al. (1997) model and the six refraction lines. The refraction lines predominately sample three volumes of the Brocher 3D model, so the depths from the Brocher model are clustered at 0.08, 0.70, and 1.60 km: the large diamonds with error bars show the average ± one standard deviation for each cluster. The line shows the regression of $z_{3.2}^{R}$ on $z_{3.2}^{B}$ used to correct the depths from the Brocher 3D model.

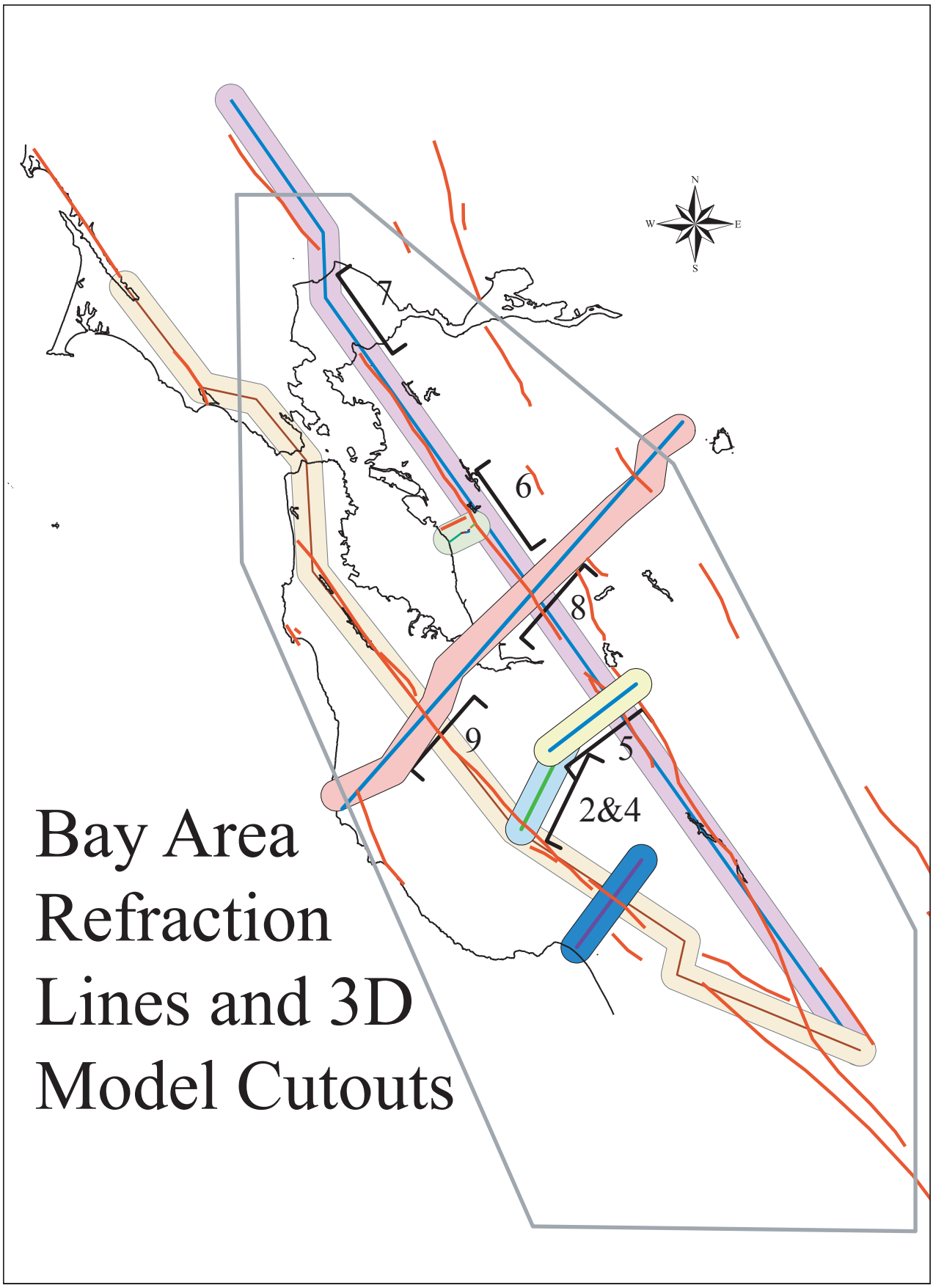
N
W
E
S
7
6
8
9
5
2&4
Bay Area
Refraction
Lines and 3D
Model Cutouts

Figure 1

Los Gatos S-Wave Inversion (Catchings et al., 2004)

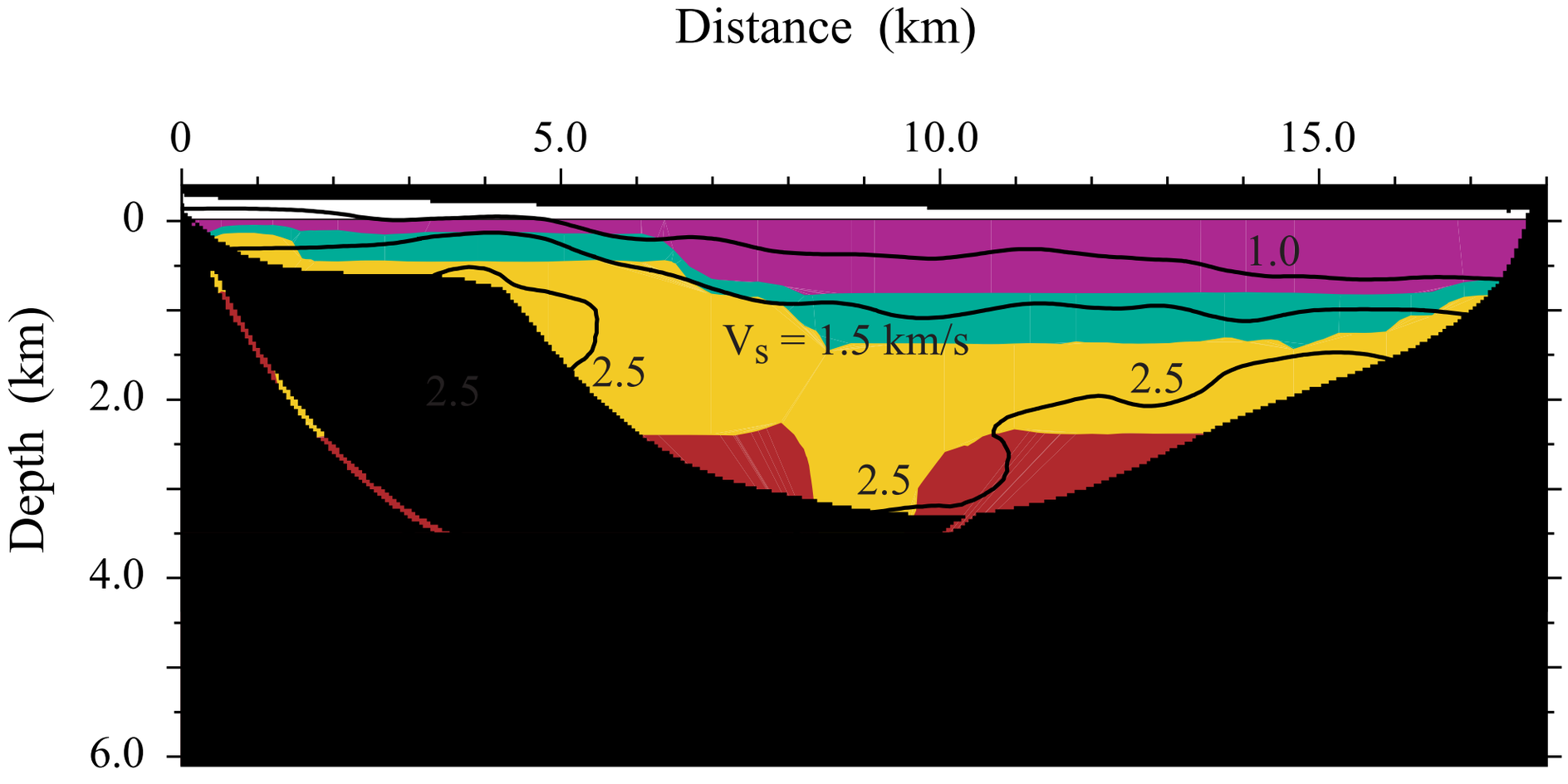

Brocher et al. (1997) 3D model in solid colors

Figure 2

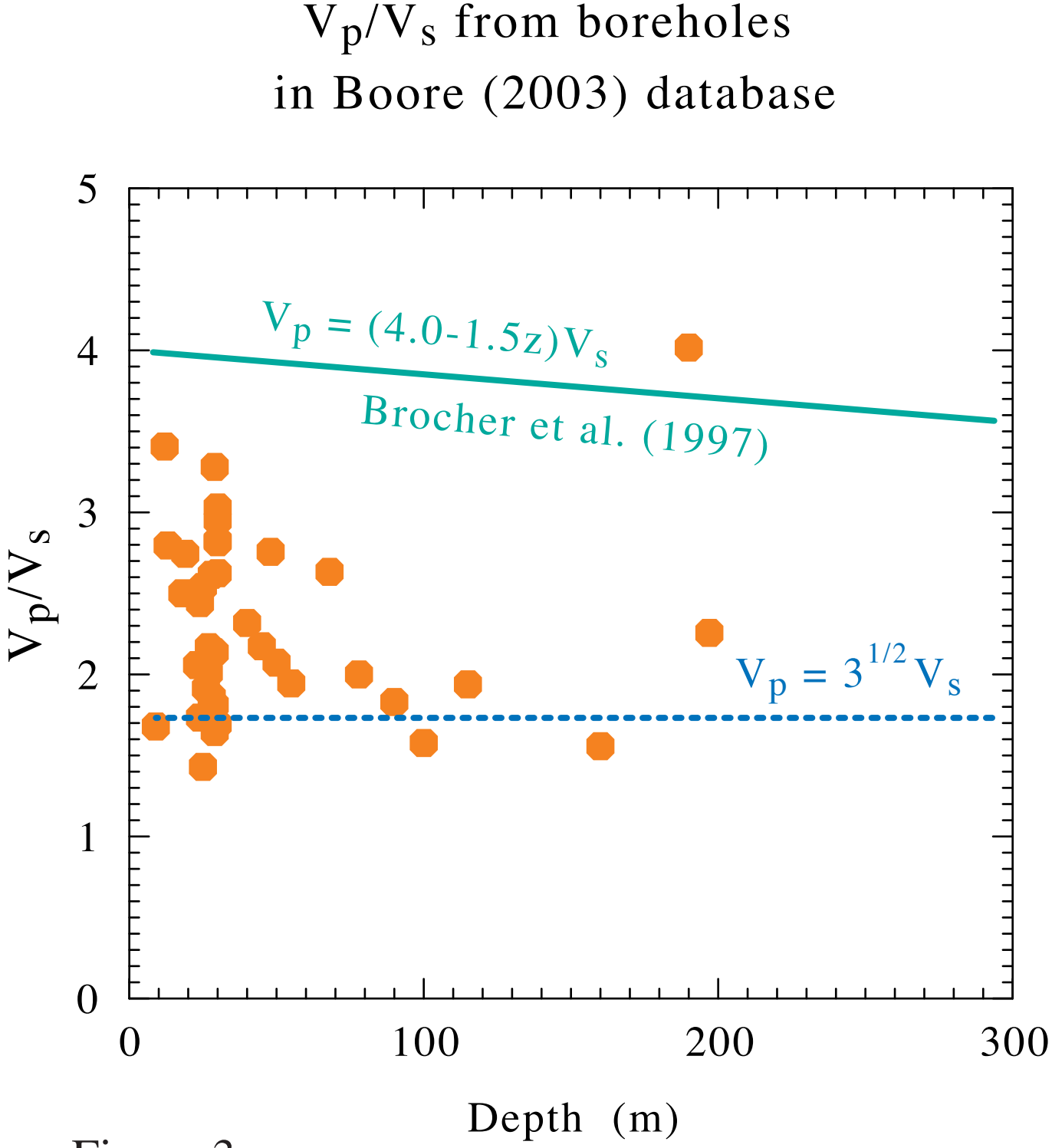
V_p/V_s from boreholes
in Boore (2003) database
$V_p = (4.0\text{-}1.5z)V_s$
Brocher et al. (1997)
$V_p = 3^{1/2}V_s$
V_p/V_s
Depth (m)
0
1
2
3
4
5
0
100
200
300

Figure 3

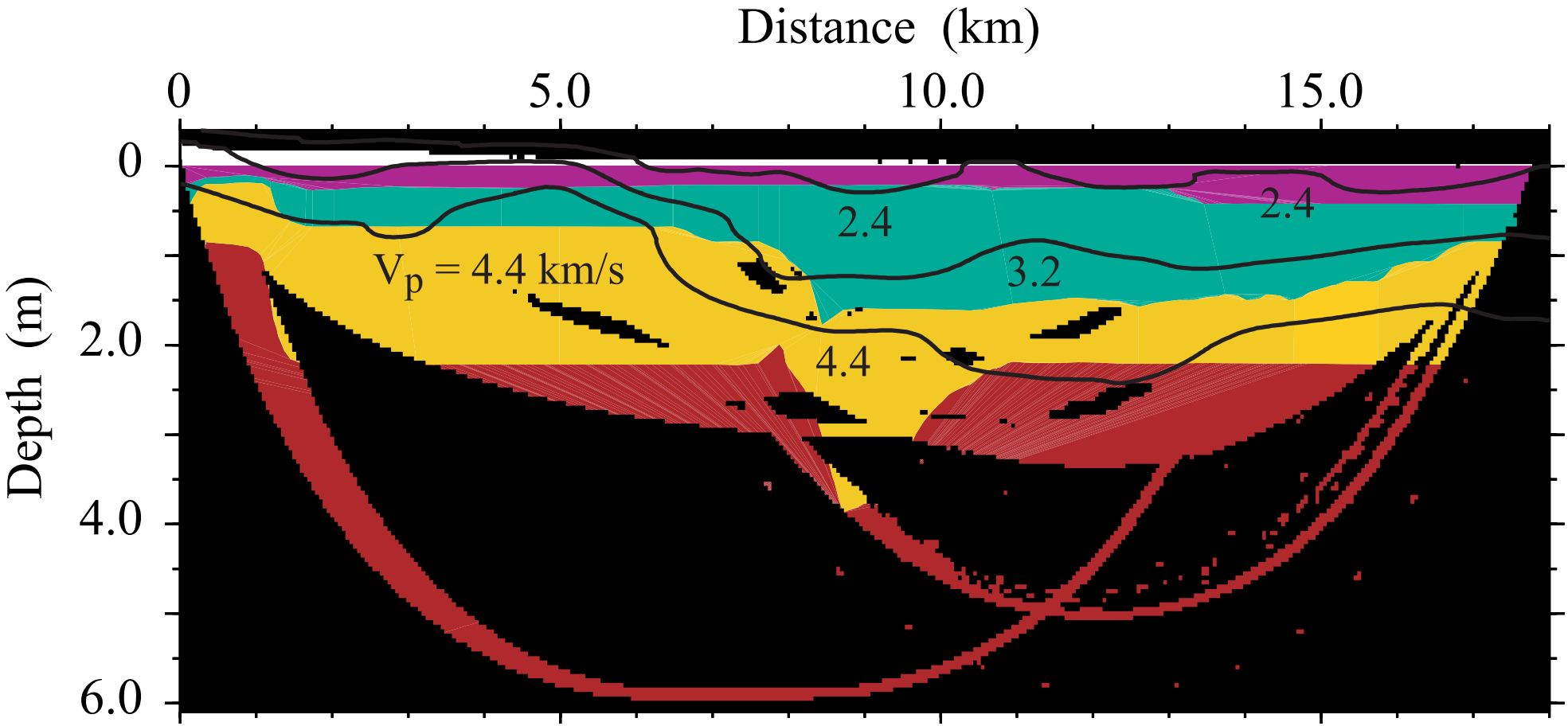
Los Gatos Inversion 1025 (Catchings et al., 2004)
Distance (km)
0
5.0
10.0
15.0
Depth (m)
0
2.0
4.0
6.0
2.4
2.4
3.2
4.4
V_p = 4.4 km/s
Brocher et al. (1997) 3D model in solid colors

Figure 4

Evergreen Basin Inversion (Catchings et al., 2004)

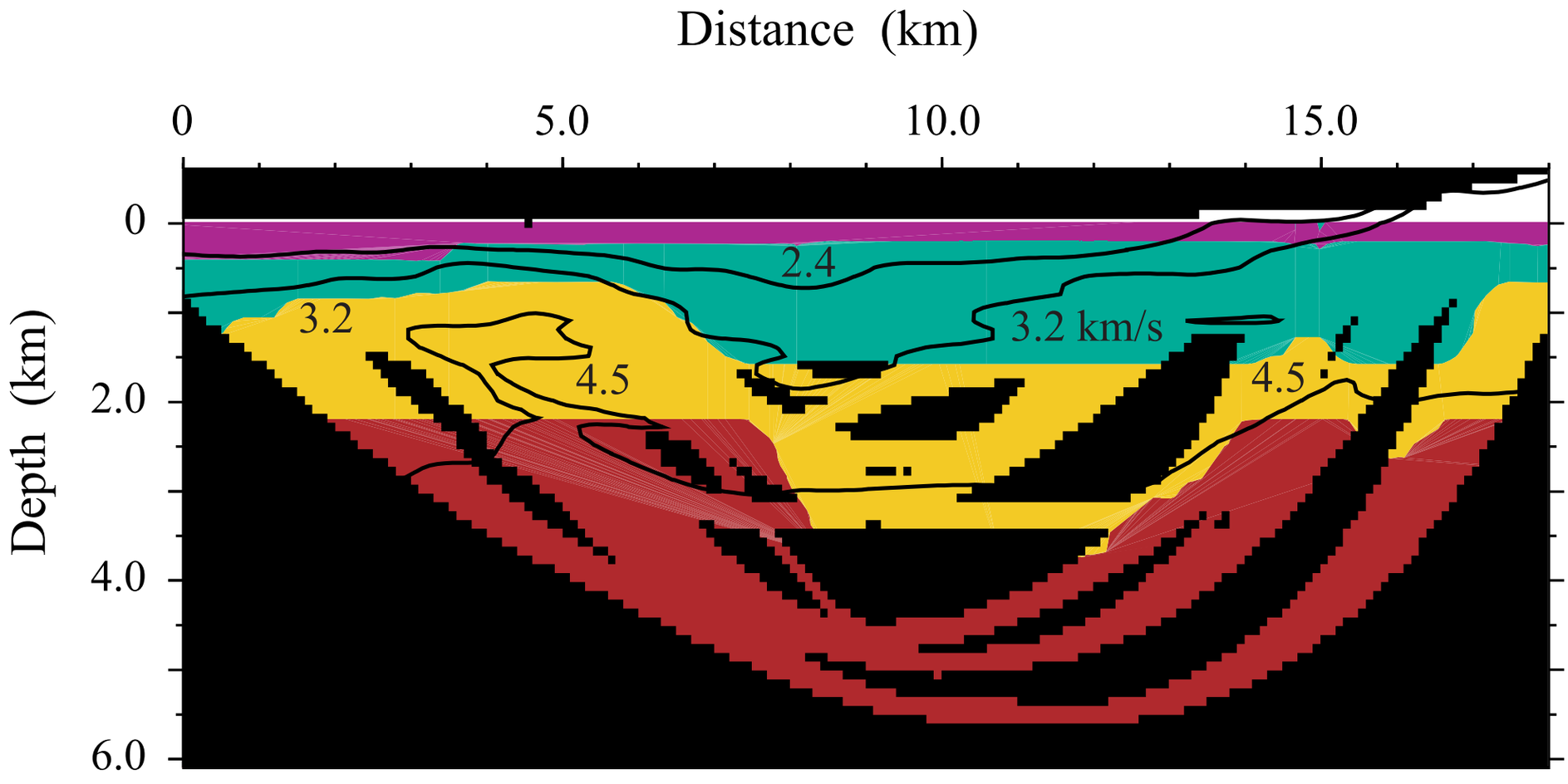

Brocher et al. (1997) 3D model in solid colors

Figure 5

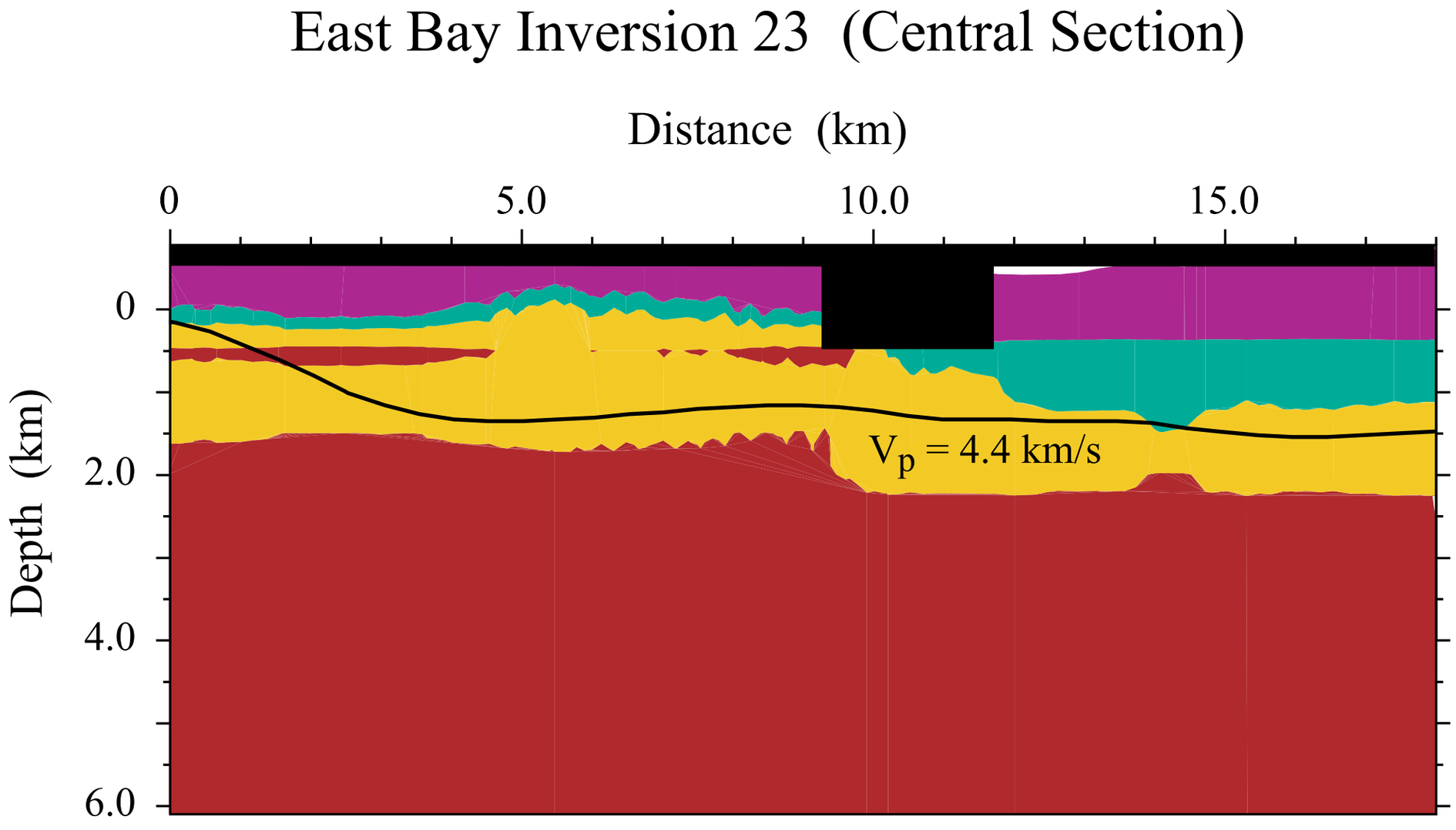

Brocher et al. (1997) 3D model in solid colors

Figure 6

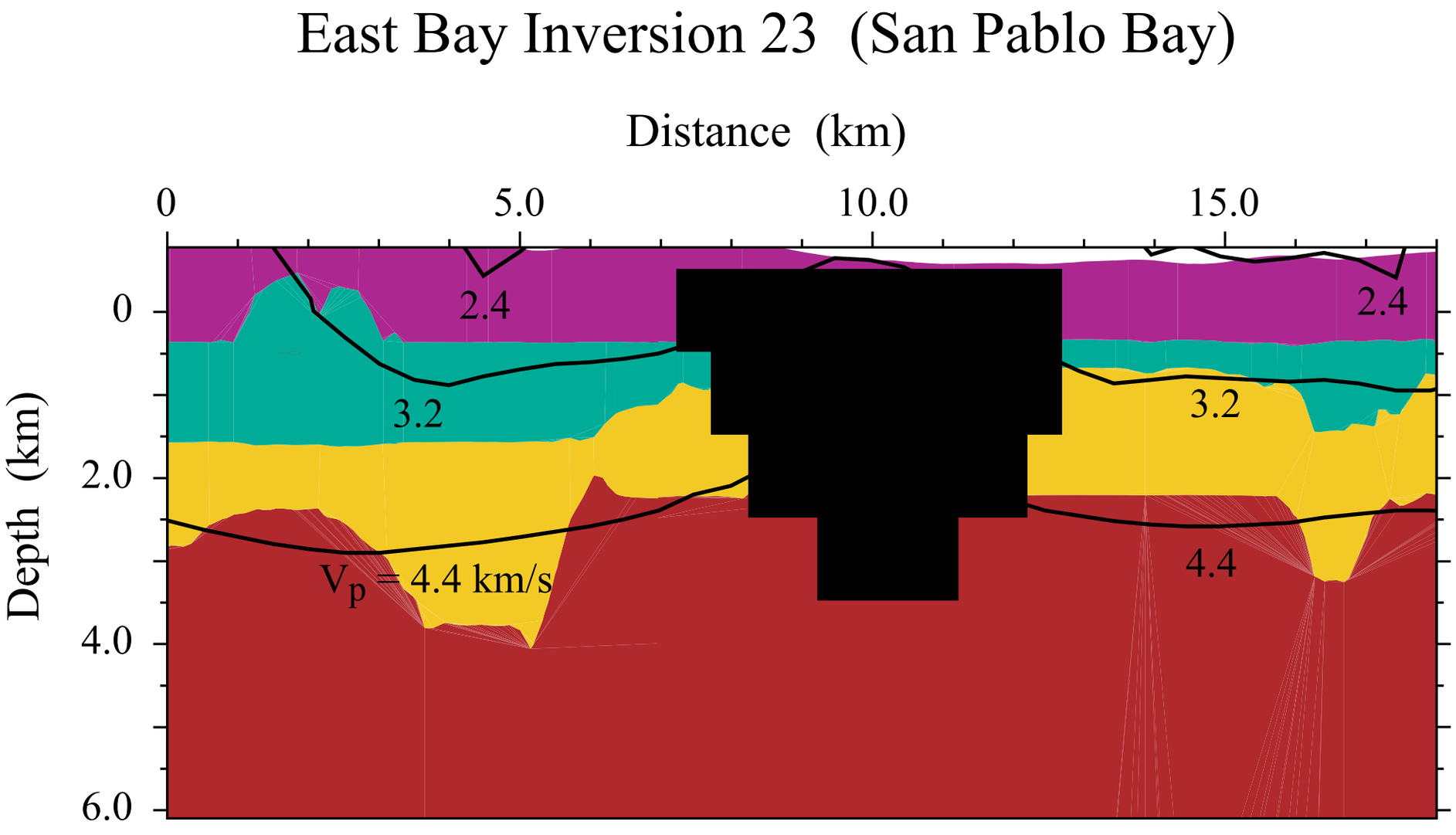

Brocher et al. (1997) 3D model in solid colors

Figure 7

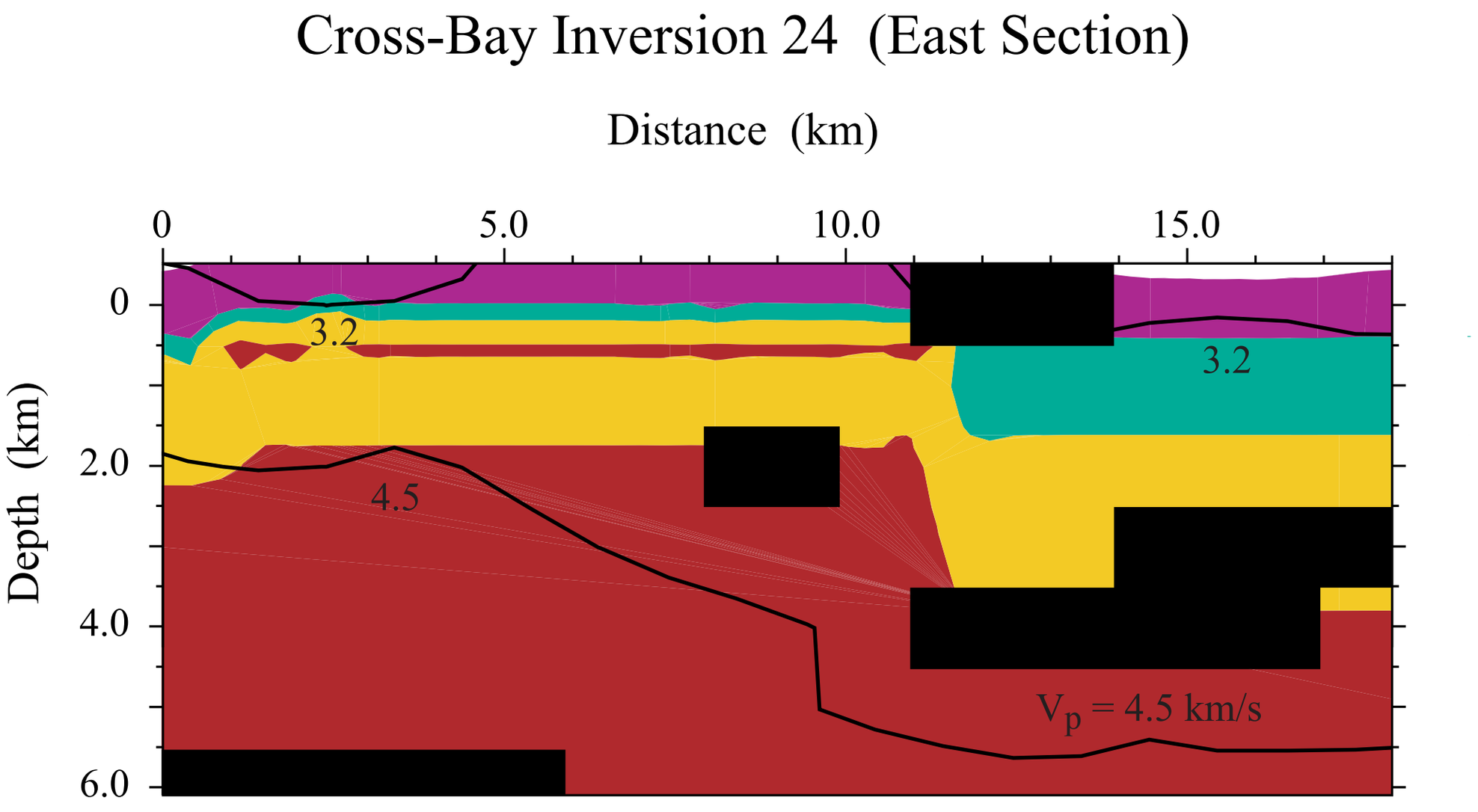

Brocher et al. (1997) 3D model in solid colors

Figure 8

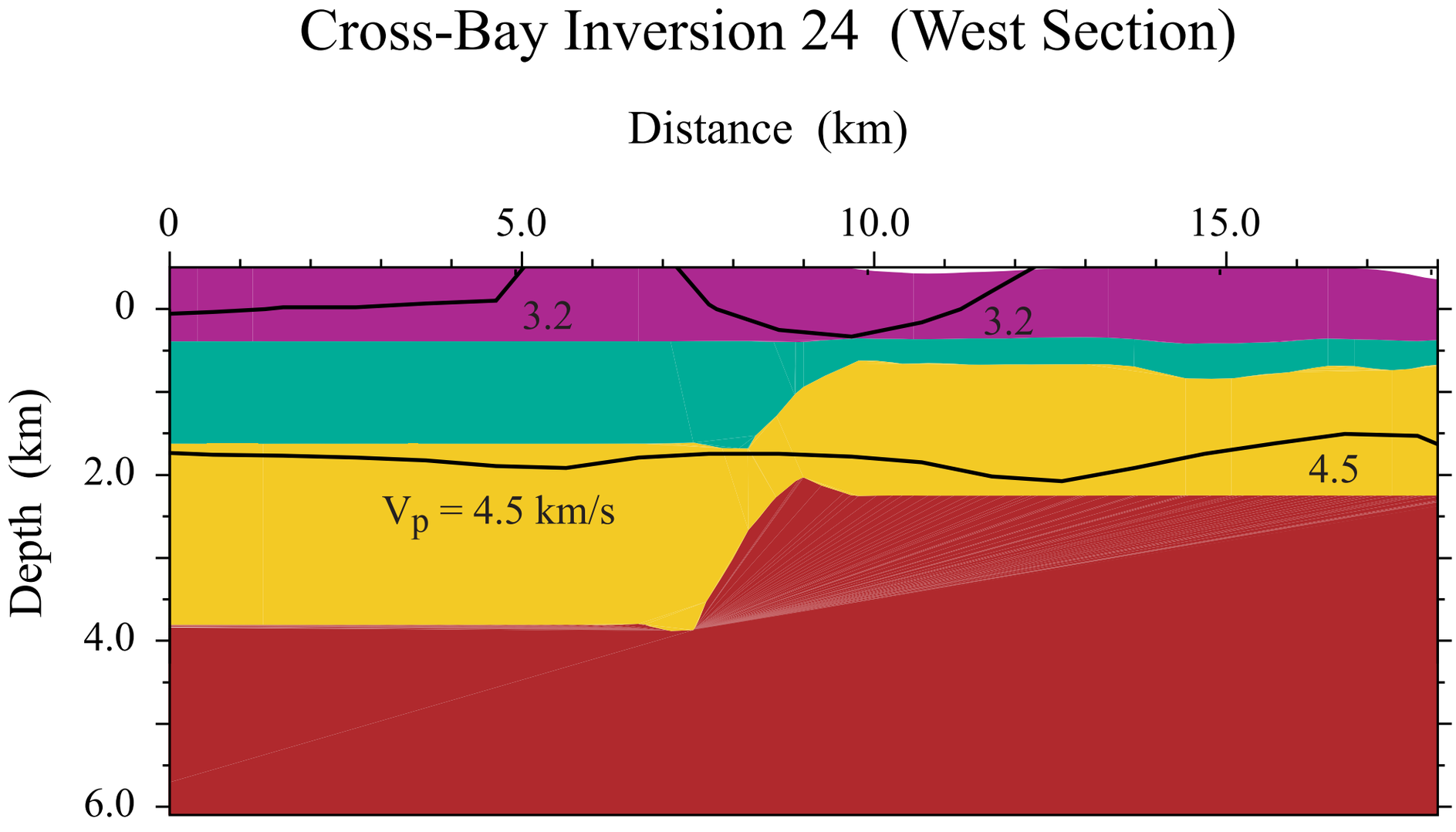

Brocher et al. (1997) 3D model in solid colors

Figure 9

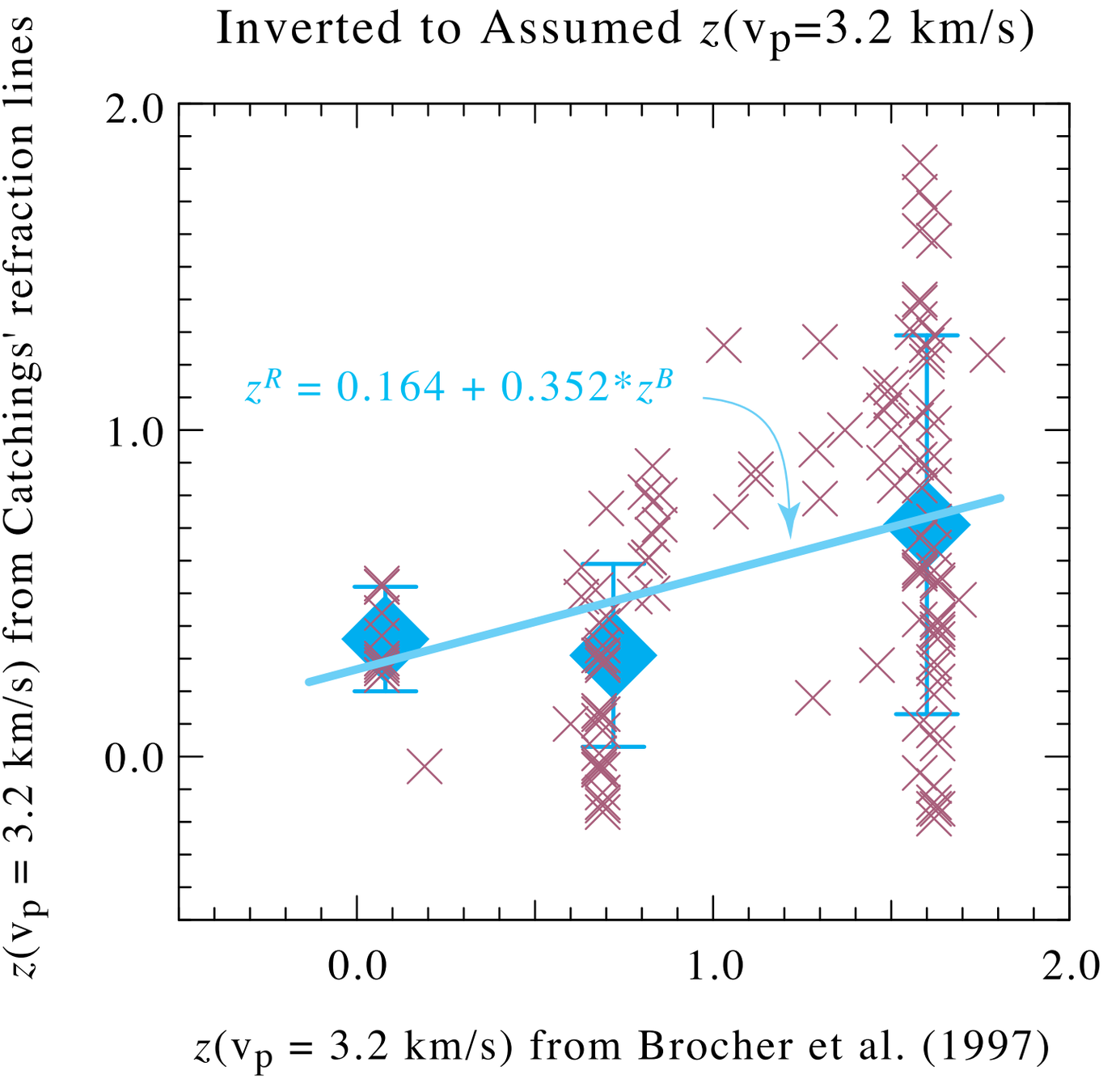
Inverted to Assumed $z(v_p=3.2$ km/s)
$z^R = 0.164 + 0.352*z^B$
2.0
1.0
0.0
0.0
1.0
2.0
$z(v_p = 3.2$ km/s) from Catchings' refraction lines
$z(v_p = 3.2$ km/s) from Brocher et al. (1997)

Figure 10

Appendix
P-Wave Velocity Structures for 6 Bay Area Refraction Lines

This Appendix locates the six refraction lines conducted by Catchings et al. in 1991, 1993, 2000, and 2003. Four of these six lines were shot in 1991-93: the Peninsula line, running from Hollister to Inverness, the East Bay line, running from Hollister to Santa Rosa, the Cross Bay line, running from Ana Nuevo to Livermore, and the Loma Prieta line. The last two lines were shot in 2000 and 2003: the Los Gatos and Evergreen lines together run from Los Gatos to Alum Rock Park, crossing the entire San Clara Valley.

The receiver locations and shot points for the 1991-93 lines are shown in Figure A1, along with the receiver locations for the 2000 and 2003 lines. The P-wave velocity structures obtained by tomographic inversion of these six refraction lines are shown in Figures A2-A6. These refraction results are presently being combined into a fence diagram that will be posted on the Earthquake Team web-site at http://quake.usgs.gov.

Bay Area Refraction Profiles

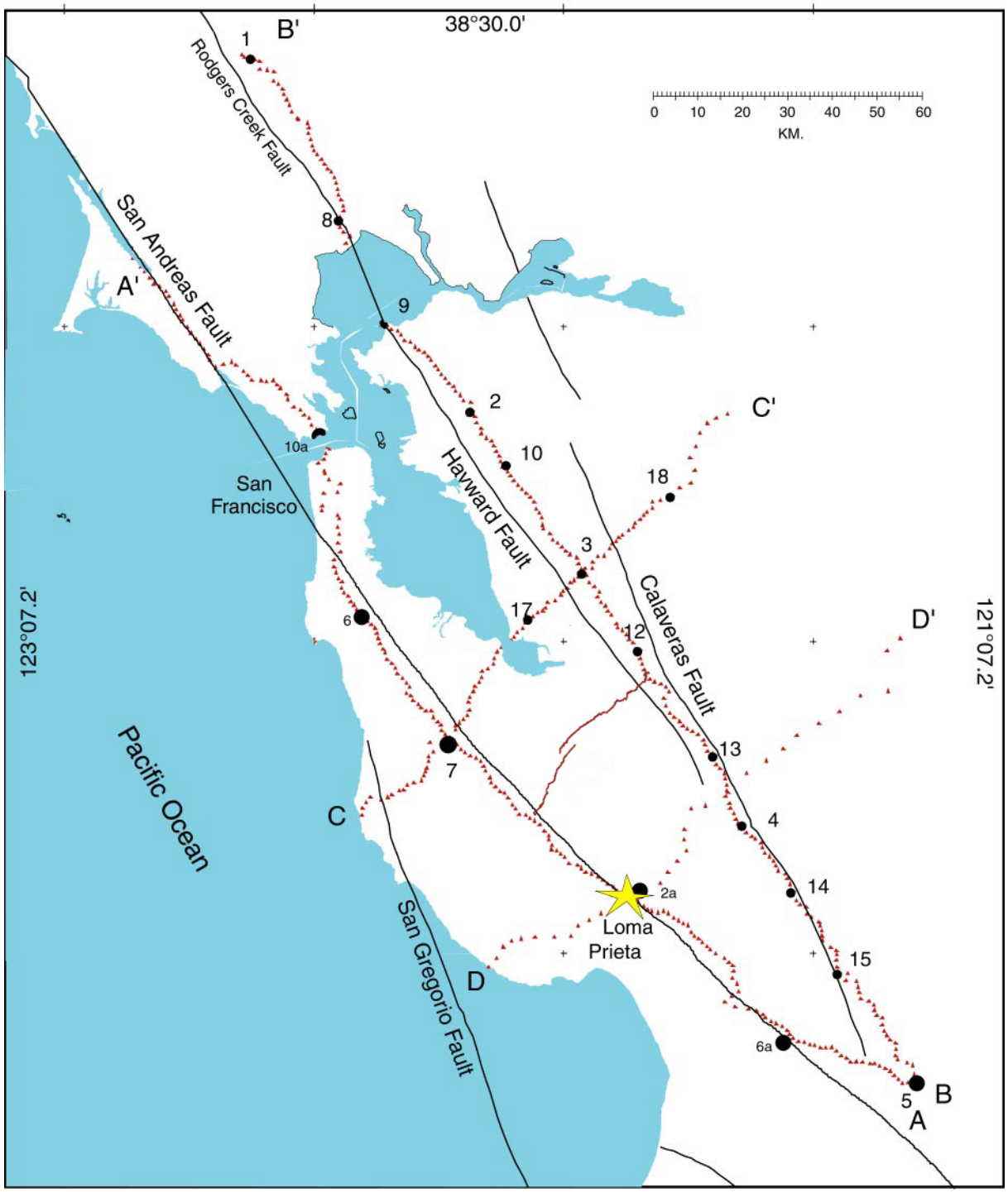

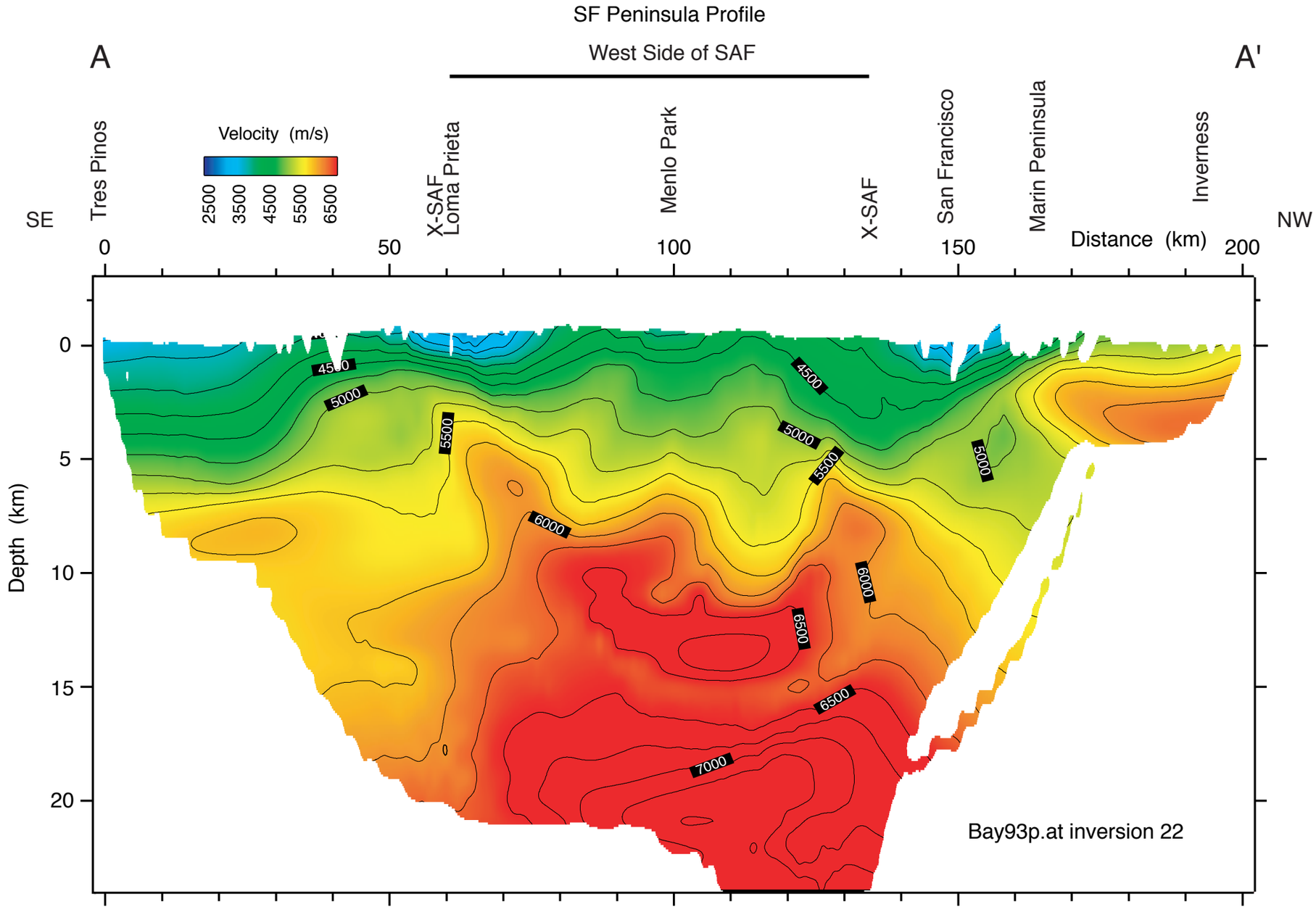
SF Peninsula Profile
West Side of SAF
A
A'
SE
NW
Tres Pinos
X-SAF
Loma Prieta
Menlo Park
X-SAF
San Francisco
Marin Peninsula
Inverness
Velocity (m/s)
2500
3500
4500
5500
6500
0
50
100
150
200
Distance (km)
Depth (km)
0
5
10
15
20
4500
5000
5500
6000
6500
7000
Bay93p.at inversion 22

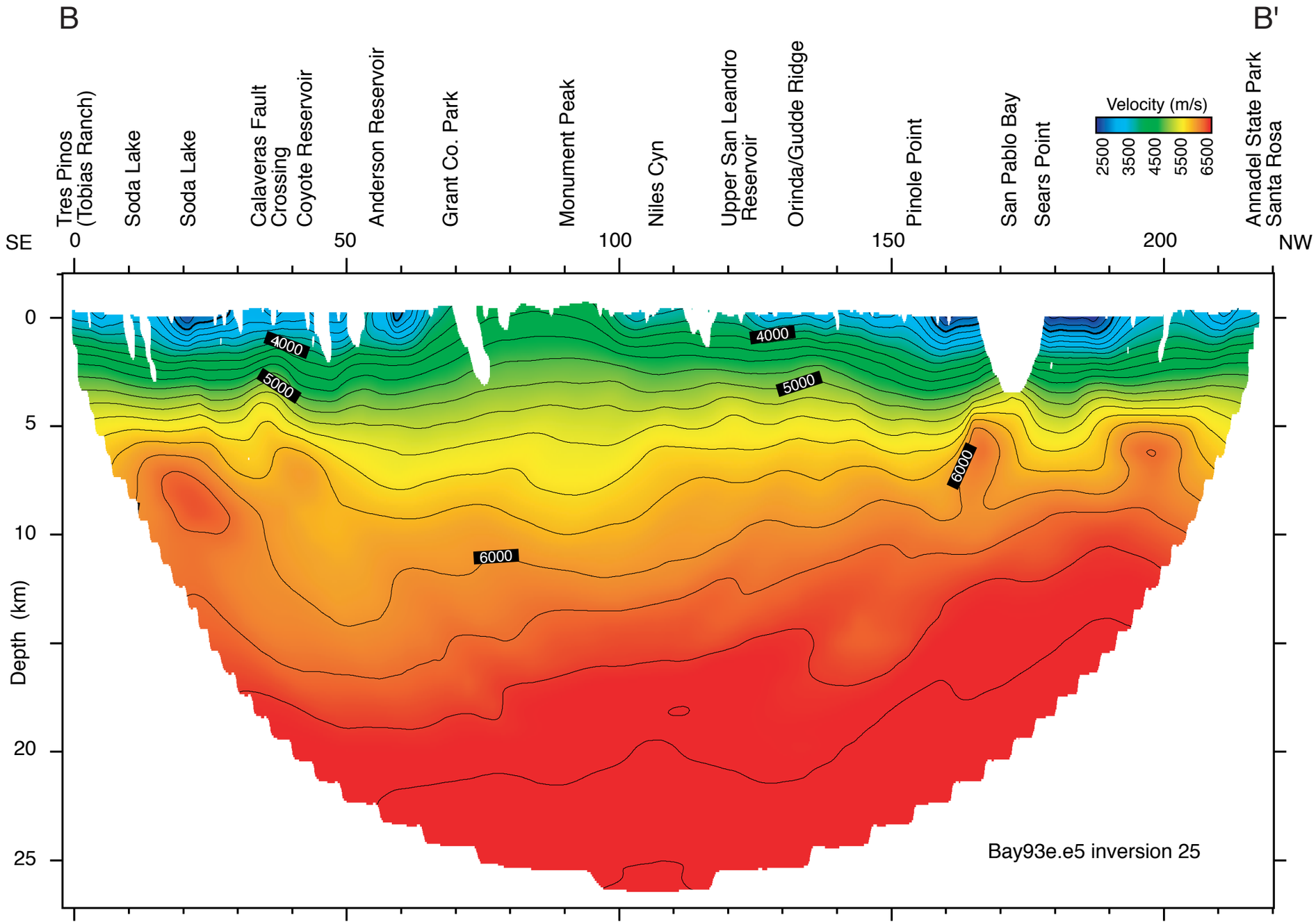
B
B'
Tres Pinos (Tobias Ranch)
Soda Lake
Soda Lake
Calaveras Fault Crossing
Coyote Reservoir
Anderson Reservoir
Grant Co. Park
Monument Peak
Niles Cyn
Upper San Leandro Reservoir
Orinda/Gudde Ridge
Pinole Point
San Pablo Bay
Sears Point
Annadel State Park Santa Rosa
Velocity (m/s)
2500
3500
4500
5500
6500
SE
NW
0
50
100
150
200
Depth (km)
0
5
10
20
25
4000
5000
6000
Bay93e.e5 inversion 25

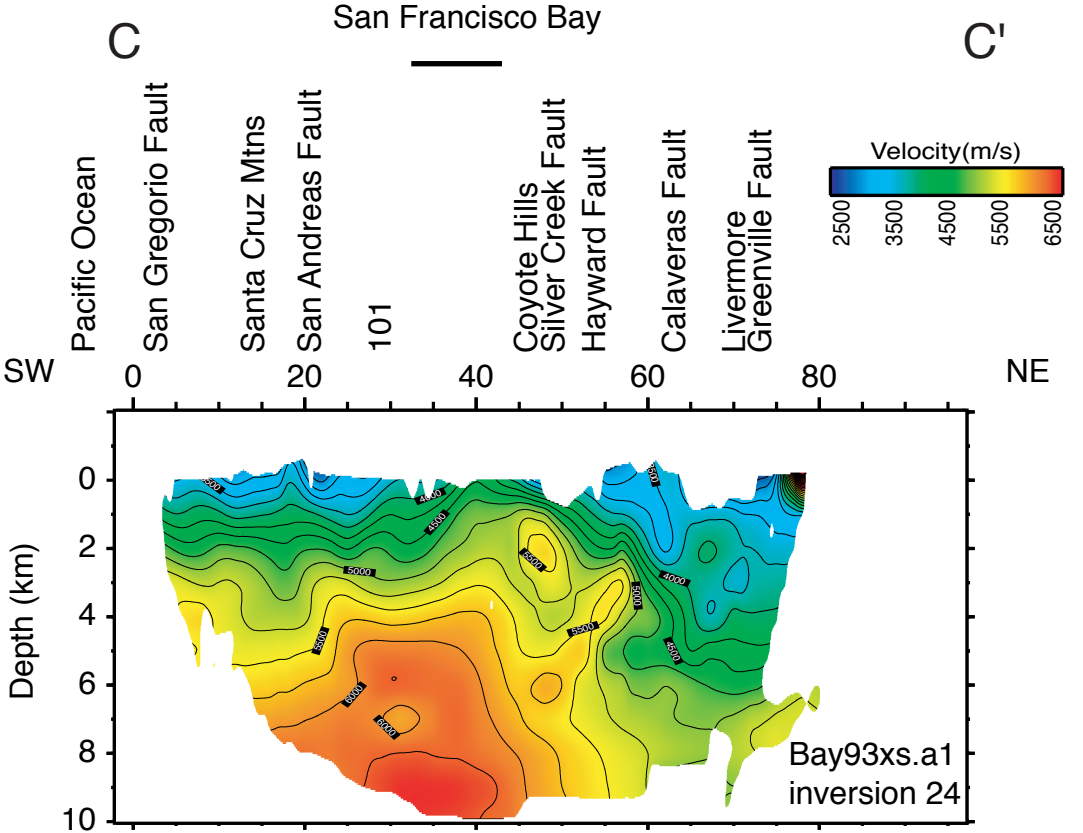
C
San Francisco Bay
C'
Pacific Ocean
San Gregorio Fault
Santa Cruz Mtns
San Andreas Fault
101
Coyote Hills
Silver Creek Fault
Hayward Fault
Calaveras Fault
Livermore
Greenville Fault
Velocity(m/s)
2500
3500
4500
5500
6500
SW
NE
0
20
40
60
80
Depth (km)
0
2
4
6
8
10
Bay93xs.a1
inversion 24

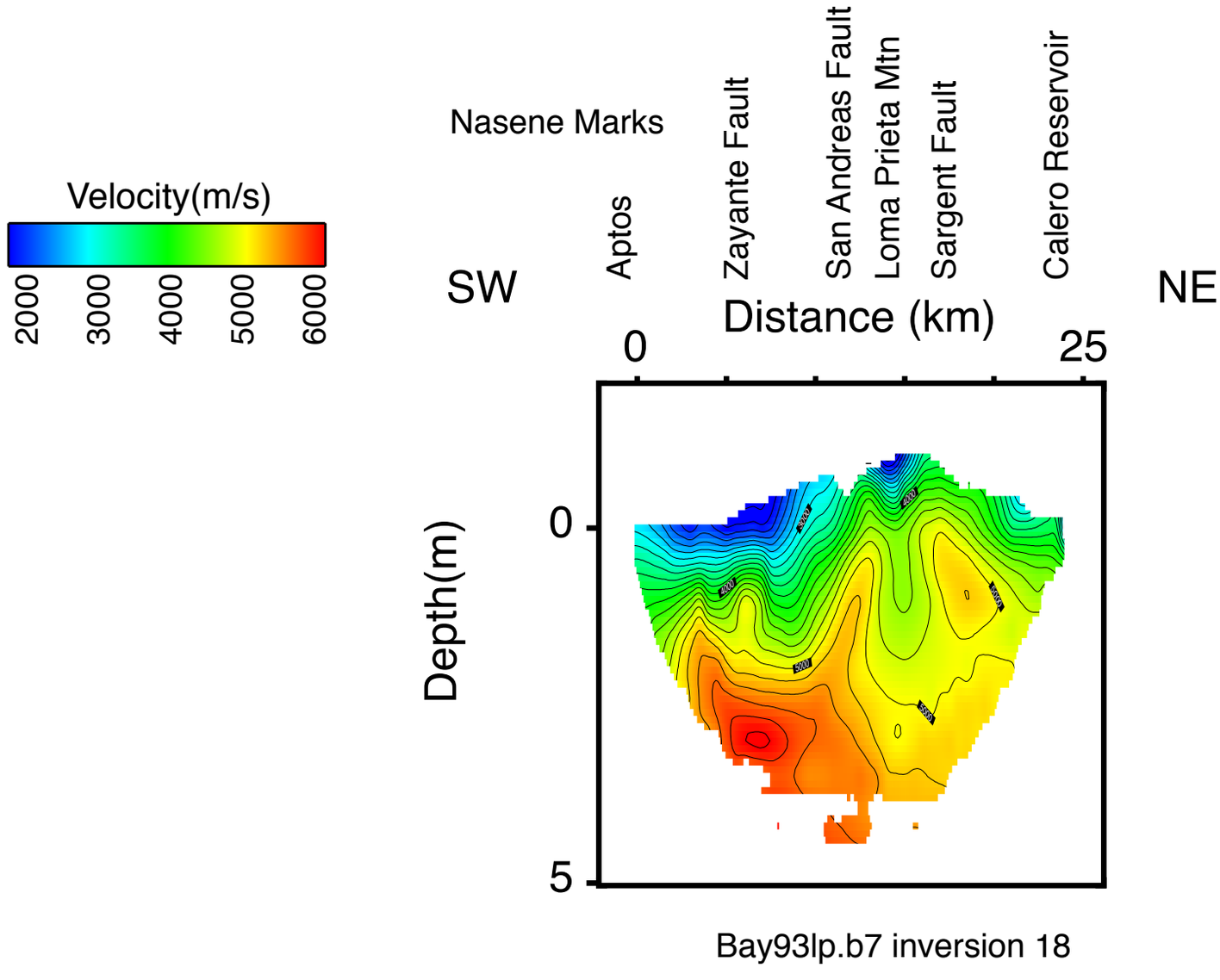
Velocity(m/s)
2000
3000
4000
5000
6000
Nasene Marks
Aptos
Zayante Fault
San Andreas Fault
Loma Prieta Mtn
Sargent Fault
Calero Reservoir
SW
NE
Distance (km)
0
25
Depth(m)
0
5
Bay93lp.b7 inversion 18

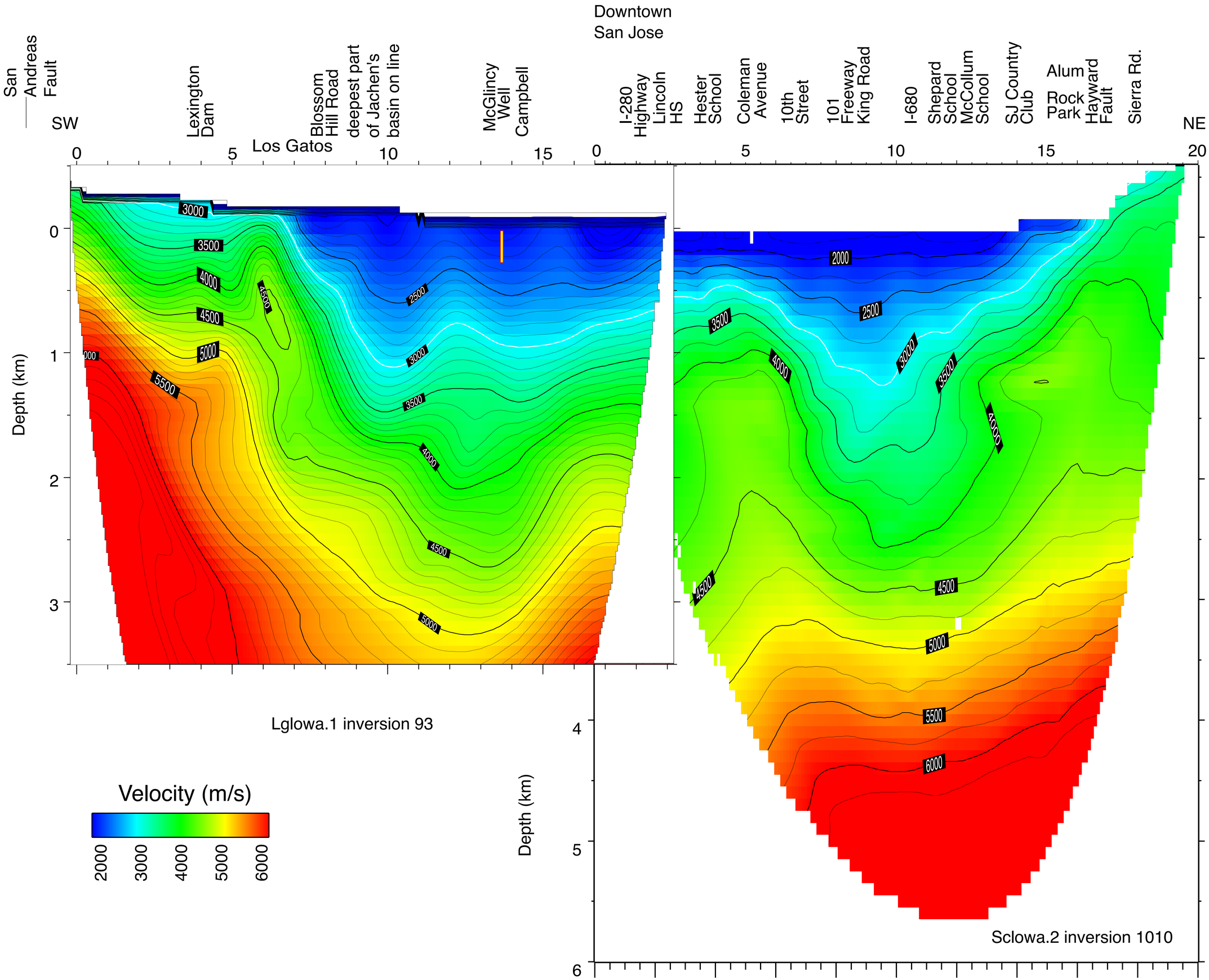
San Andreas Fault
SW
Lexington Dam
Los Gatos
Blossom Hill Road
deepest part of Jachen's basin on line
McGlincy Well
Campbell
Downtown San Jose
I-280 Highway
Lincoln HS
Hester School
Coleman Avenue
10th Street
101 Freeway
King Road
I-680
Shepard School
McCollum School
SJ Country Club
Alum Rock Park
Hayward Fault
Sierra Rd.
NE
Depth (km)
Lglowa.1 inversion 93
Sclowa.2 inversion 1010
Velocity (m/s)
2000
3000
4000
5000
6000